

Extending Structural Causal Models for Autonomous Embodied Systems

Rhys P. M. Howard¹, Lars Kunze²,

¹Oxford Robotics Institute, Dept. of Eng. Sci., University of Oxford, 17 Parks Road, Oxford, OX1 3PJ, UK

²Bristol Robotics Laboratory, T-Block, UWE Bristol, Bristol, BS16 1QY, UK

rhysward@live.com, lars.kunze@uwe.ac.uk

Abstract

In this work we aim to bridge the divide between autonomous embodied systems and causal reasoning. Autonomous embodied systems have come to increasingly interact with humans, and in many cases may pose risks to the physical or mental well-being of those they interact with. Meanwhile causal models, despite their inherent transparency and ability to offer contrastive explanations, have found limited usage within such systems. As such, we first identify the challenges that have limited the integration of structural causal models within autonomous embodied systems. We then introduce a number of theoretical extensions to the structural causal model formalism in order to tackle these challenges. This augments these models to possess greater levels of modularisation and encapsulation, as well presenting a constant space temporal causal model representation. While not an extension itself, we also prove through the extensions we have introduced that dynamically mutable sets can be captured within structural causal models while maintaining a form of causal stationarity. Finally we introduce two case study architectures demonstrating the application of these extensions along with a discussion of where these extensions could be utilised in future work.

Code — <https://github.com/cognitive-robots/SimCARSv2>

1 Introduction

We continue to see ever greater integration of AI into systems that physically interact with us and the world around us. This has coincided with the widespread emergence of deep neural networks and other black box methodologies that are limited in their ability to provide transparency and grounded explanations (von Eschenbach 2021; Adadi and Berrada 2018; Gunning and Aha 2019). We propose that since explanations have long been tied to causality within philosophy (Salmon 1998), psychology (Gerstenberg 2022), and statistics (Pearl 2009), a high-resolution causal model-based approach to developing AI systems can allow us to engineer systems that are both explainable and transparent.

In this paper we aim to bridge the gap in literature that exists between autonomous embodied systems (AESs) — e.g. robots, autonomous driving — and causal reasoning. We define an AES as any system in which an agent determines its own decisions / behaviour, and has a physical manifestation or body through which it interacts with the world.

Despite the identified merits of incorporating causality into these systems (Gadd et al. 2020; Hellström 2021), there exists relatively few that utilise an architecture built directly upon causal models, as discussed in Sec. 2. We argue that this is largely due to causal models being considered an external tool with which to examine data or systems, rather than the basis of such systems. Here we explore the challenges associated with integrating AESs with structural causal models (SCMs) (Pearl 2009) before presenting a series of extensions in order to address these challenges. We demonstrate these extensions through two case studies, focusing upon architectures built for the domains of autonomous driving and service robotics respectively. We finalise with a discussion of how future work might build upon or utilise these extensions.

2 Related Work

As discussed in the previous section, causality has been identified as a critical component in explainable artificial intelligence (XAI) (von Eschenbach 2021; Adadi and Berrada 2018; Gunning and Aha 2019), and more specifically explainable robotics (Hellström 2021), allowing us to understand why decisions are made as they are. This in turn can be utilised in establishing accountability (Poehhacker and Kacianka 2021) or improving performance via self-extension (Marfil, Bustos, and Bandera 2024). In this work we focus upon the integration of SCMs with AESs specifically due to the transparency they offer versus black-box methodologies such as neural networks (NNs). While causal modelling and discovery approaches have utilised methods such as variational autoencoders (Yang et al. 2021) and attention-based convolutional NNs (Nauta, Bucur, and Seifert 2019) to provide some level of explanation, they are at best able to ground such explanations in Granger causality (Granger 1969). In an age where governments are moving to regulate artificial intelligence and legal cases surrounding it increase, we therefore aim to provide a means of constructing causally-grounded architectures with maximal transparency.

A promising direction for the integration of AESs and SCMs considers the integration of Markov decision processes (MDPs) with SCMs (Nashed et al. 2023; Cannizzaro and Kunze 2023; Triantafyllou and Radanovic 2023). MDPs are frequently used to model agents in AESs and thus these works represent a notable step in the right direction. How-

ever, of the aforementioned approaches of both Nashed *et al.* (2023), and Cannizzaro & Kunze (2023) focus upon simple grid-world problems that concern only a single agent; while Triantafyllou & Radanovic (2023) do not focus upon embodied agents, and only capture agent interactions in terms of taking turns in two-player games.

Other approaches have utilised causal models similar to SCMs such as causal Bayesian networks for explanation, prediction and proactive behaviour in robotics (Diehl and Ramirez-Amaro 2023), but these also focus upon a specific scenario considering a single agent. Wich *et al.* (2022) specify an SCM to identify key factors in hand selection when executing manipulation tasks, but once again said model is highly specialised to this purpose and only considers a single agent. Madumal *et al.* (2020) present a high-level SCM that seems to more generally capture agents playing *StarCraft II* outside of a specific scenario, however each agent is represented via its own SCM rather than as part of a complete model and the system is disembodied. Maier *et al.* (2024) provides a more detailed SCM with some modularity that even captures interactions between vehicles, the main limitation is that the SCM is specific to a simple advanced driver assistance system scenario.

There has also been some interest in representing ordinary differential equations through SCMs in order to capture dynamic systems (Mooij, Janzing, and Schölkopf 2013; Bongers *et al.* 2021), however these methods have yet to be applied to autonomous embodied systems to the best of our knowledge. These works achieve the representation of these equations in SCMs via the use of cycles, and for this reason we have opted to avoid utilising these techniques within this work, as our proposed formalisms and their associated case study architectures are effectively acyclical — a common requirement of many causal reasoning techniques.

We also set ourselves apart from work concerning the active discovery of causal relationships. Castri *et al.* (2022) covers the discovery of causal relationships between agent variables within a multi-agent pedestrian environment. While such work can produce a causal graph, it is substantially more difficult to identify the structural equations pertaining to high-level relationships, and in some cases AES agent data may prove unsuitable for such techniques (Howard and Kunze 2023b). Instead we argue for utilising well established knowledge regarding kinematics / dynamics, control systems, and planning in order to design the causal graph and structural equations.

We argue this work provides the first comprehensive set of extensions that address challenges hampering the integration of SCMs into AESs. Although we cover these challenges in depth in Sec. 4, obstacles relating to the temporal nature of AESs, as well as the lack of general system representation have been identified in previous works as reasons for avoiding SCM usage (Gyevnar *et al.* 2024). In presenting our extensions, we aim to enable greater use of SCMs within AESs and foster discourse over remaining obstacles to such use.

3 Structural Causal Models

A popular means of representing causal relationships between variables is the SCM (Pearl 2009; Bareinboim, For-

ney, and Pearl 2015). A SCM $\mathcal{M} = \langle \mathcal{U}, \mathcal{V}, \mathcal{F}, P(\mathcal{U}) \rangle$ is comprised of both endogenous variables \mathcal{V} and exogenous variables \mathcal{U} . Endogenous variables are those the model aims to describe and derive their values from the structural equations given in \mathcal{F} . Meanwhile exogenous variables capture independent external factors that are not explicitly modelled, and thus derive their values from the joint probability distribution $P(\mathcal{U})$. We additionally introduce the function $Pa(\cdot)$ which gives the parent variables of an endogenous variable based upon its associated structural equation.

Temporal Extension Many domains, including those relating to AESs make use of time series data or similar. Thus adaptations have been introduced to capture the temporal elements of causality in SCMs, with Peters *et al.* (2017) giving a comprehensive overview of this in the context of temporal causal discovery.

To summarise methods of temporally extending SCMs, we cover three common representations here:

- **Summary Graph:** Utilises the original set of variables and establishes a causal link between two variables if there is a causal link between said variables regardless of the time lag.
- **Full Time Graph:** Simply replicates each variable for the entire time period being modelled, thus allowing causal relations to be represented between any pair of variables each associated with any time step.
- **Window Graph:** Has $(\Delta T_{max} + 1)$ copies of each variable in order to represent causal relations with a maximum time lag of ΔT_{max} . This relies upon the causal relations between the relative time steps of the variables within the window graph being consistent across all time steps modelled, i.e. causal stationarity (Runge 2018).

4 Challenges for SCM Integration in Autonomous Embodied Systems

4.1 Modularisation & Encapsulation

While SCM use in AESs remains rare, those works that do utilise SCMs typically either utilise a single monolithic SCM, or several entirely independent SCMs. Furthermore it is rare to store the data relating to an SCM within the structure of an SCM itself. This is a reasonable approach for experimental settings or when working in data science. However, effective system design would suggest we should aim to modularise & encapsulate SCMs in order to minimise repetitions in the graphical structure, restrict data access based upon system design, and cater each module to a particular aspect of the system (Scott 2009). While these are desirable qualities in system design across domains, AESs have in particular shown a preference for modular libraries which are easily ported and integrated across systems, the best showcase of this being the robot operating system (ROS) (Macenski *et al.* 2022).

SCMs are to some degree already modular by nature (Pearl 2009), as a causal graph may be cut and endogenous variables replaced with exogenous. However this leaves system designers few options for hiding or exposing exogenous variables, nor a mechanism for separating SCM modules

once connected. We implement these capabilities primarily through the socket variables described in Sec. 5.5. Furthermore, in terms of controlling access to data / variables within the SCM modules themselves, this can be specified by the wrapper provided for the SCM (e.g. class accessors). This in turn requires the encapsulation of data within SCMs, something achieved through the buffer variables documented in Sec. 5.4.

4.2 Constant Space Representation of Time Series

Window graphs offer a compact representation of temporally lagged causal relationships, particularly for AESs, which often assume the Markov property — i.e. the next state only depends upon the current state. However, even the window graph representation still requires one to roll-out the graph during inference to cover the relevant time period. This can lead to the rolled-out graph taking up a great deal more space than the initial window graph, not to mention that inferences over different time periods usually each require their own independent roll-out. This becomes especially complicated when one wishes to use the generative properties of SCMs to counterfactually simulate different outcomes, creating separate branches for each inferred history.

Lastly, the window graph roll-outs represents a problem for the design of SCM wrappers. If the window graph for an SCM captures the underlying model of the system then it is unclear whether performing a roll-out should mutate the original SCM window graph within the wrapper, or whether the roll-out operation should return a newly rolled-out SCM to manage separately. The former means losing the original window graph SCM, while the latter means managing a potentially large number of SCMs, neither of which is ideal.

Our solution is to utilise a recursive SCM formulation combined with the ideas of an SCM variable context and temporal variables introduced in Sec. 5.2 & 5.3. This ties in with the addition of buffer variables introduced in Sec. 5.4 as these variables utilise the aforementioned variable context in order to store data time-indexed within the SCM itself.

4.3 Arbitrary Number of Agent Interactions

When operating within their environments AESs belonging to certain domains — such as those considered in the case studies — will interact with various agents. The number and nature of these agents will often vary, thus an SCM capturing an AES should allow the handling of dynamic set of values. While the structural equations of an SCM can derive an output from an input set, the greater issue is being able to dynamically formulate such a set within an SCM. In instances where this set is derived directly from observation, this can simply be captured via an exogenous variable. However, we are considering a dynamic set of agents we may also wish to model within the SCM. In particular, causal methods grounded in intentionalism (Dennett 1971) may wish to utilise a theory of mind for other agents when making counterfactual inferences.

We solve this by proving that through a combination of our proposed extensions it is possible to capture a dynamic

set of agents while maintaining a form of causal stationarity Sec. 5.6.

5 Extending SCMs for Autonomous Embodied System

5.1 Structural Equations with Side-Effects

Before we can properly introduce any extensions to the SCM formalism, we first need to describe the process of integrating side-effects into the structural equations of an SCM. Side-effects in this context of this work refer to computations that occur beyond the purely mathematical calculations of structural equations (e.g. I/O, memory). In order to incorporate this into the SCM formalism, we take a similar approach to that typically observed in functional programming paradigms by utilising monadic actions (Wadler 1992). The use of monads is widely documented and thus only a succinct description is given here. A monad is comprised of: a type constructor $\mathfrak{M}(\cdot)$; a unit / return function $u_{\mathfrak{M}}(\cdot) : \tau_X \rightarrow \mathfrak{M}(\tau_X)$ which wraps a value of type τ_X with the monad type \mathfrak{M} ; and a bind function $b_{\mathfrak{M}}(\cdot) : \mathfrak{M}(\tau_X) \rightarrow (\tau_X \rightarrow \mathfrak{M}(\tau_Y)) \rightarrow \mathfrak{M}(\tau_Y)$ that applies a function to the wrapped value of the monad while propagating the monad forwards. The bind function is also occasionally denoted via a binary operator $\triangleright_{\mathfrak{M}}$ for a cleaner presentation.

5.2 Variable Context

A variable context \mathcal{C} is a set of meta-variables that are globally accessible by the structural equations of the SCM to which it belongs. Utilisation of such a concept must be handled with care, as one could inadvertently incorporate causal relationships via \mathcal{C} that would not be represented within the causal graph of the SCM. However, \mathcal{C} only captures the current time $C_T \in \mathcal{C}$ and the time step size $C_\delta \in \mathcal{C}$, and these are only used to emulate a temporal roll-out and carry out other time-related computations. Thus \mathcal{C} does not invalidate SCMs that make use of it provided they do so via the structural equations described in Sec. 5.3.

From a theoretical point of view we can utilise the well documented state monad (Wadler 1992) — denoted with \mathfrak{S} where necessary — to track the values of \mathcal{C} during inference. However, for the sake of simplicity in notation, and in order to focus upon the core contributions of this work, we will assume that \mathcal{C} is globally accessible and thus reference its meta-variables directly.

5.3 Temporal Variables

Temporal variables do not refer to a specific variable or structural equation but instead a class of endogenous variables that operate on, or with, time meta-variables. These can be further separated into variables whose computations rely upon meta-variables and previous time step (PTS) variables which establishing the temporal structure of the SCM. We will discuss the latter of these first, as they are essential to understanding temporal representation within the extended SCM formalism.

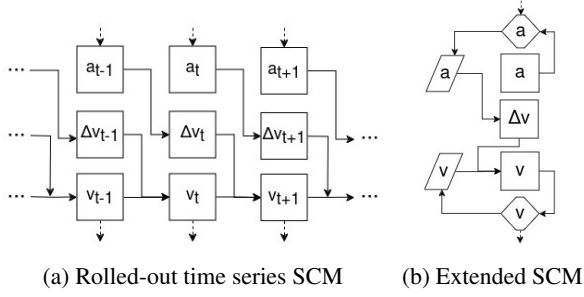


Figure 1: The SCMs depict the calculation of velocity v from acceleration a by calculating the velocity difference Δv and adding it to the velocity from the previous time step. A typical time series SCM would be coupled along with time series data, corresponding with time indexed variables — indicated via subscripts. In contrast the extended SCM representation uses PTS variables (parallelograms) and buffer variables (hexagons). These allow the SCM a fixed-size graph while still capturing causal links between time steps, in addition to providing data encapsulation.

Previous Time Step Variables We define PTS variables as a subset of endogenous variables $\mathcal{V}_\delta \subseteq \mathcal{V}$, with each PTS variable $V_\delta \in \mathcal{V}_\delta$ having an associated structural equation $f_{V_\delta} \in \mathcal{F}$ defined as follows:

$$f_{V_\delta}(V_{Pa}) = \delta_- \triangleright_{\mathfrak{S}} (\lambda \emptyset. V_{Pa}) \triangleright_{\mathfrak{S}} \delta_+ \quad (1)$$

where \emptyset denotes the empty set / value, $\delta_- : \mathfrak{S}(\emptyset)$ is a monadic value, and $\delta_+(\cdot) : \tau_{V_{Pa}} \rightarrow \mathfrak{S}(\tau_{V_{Pa}})$ is a function. Importantly δ_+ and δ_- utilise their monadic action to incremented or decremented the current time C_T of \mathcal{C} by C_δ respectively. This has the effect of shifting the current time to the previous time step, evaluating the parent variable V_{Pa} , before returning the current time to where it was initially. The function expects that the parent V_{Pa} also possesses the monad \mathfrak{S} . If this is not already the case — i.e. from V_{Pa} having PTS variable ancestors of its own — this can easily be achieved via use of the unit function $u_{\mathfrak{S}}(\cdot)$.

By utilising PTS variables we can represent temporal causal relationships in an SCM while maintaining the size and shape of the causal graph even during inference. Fig. 1 illustrates this by showing how temporal causal relations in kinematics can be captured via the introduction of recursive cycles of the causal graph, as opposed to performing a roll-out of a window graph during inference. Typically cycles would invalidate the SCM and break with assumptions made by many causal reasoning techniques. However the combination of graphical structure, PTS variables, and \mathcal{C} means that inference upon the SCM effectively emulates a roll-out while avoiding any modification to the SCMs graphical structure. Thus any casual reasoning method which can operate upon a window graph SCM should equally function upon an SCM utilising the proposed temporal representation.

Time Step Size Product / Quotient Variables Time step size product (TSSP) variables $\mathcal{V}_{\times\delta} \subseteq \mathcal{V}$ and time step size quotient (TSSQ) variables $\mathcal{V}_{\div\delta} \subseteq \mathcal{V}$ simply aim to multiply

or divide their input by the time step size C_δ respectively. Formally, we can define their functions as follows:

$$f_{V_{\times\delta}}(V_{Pa}) = V_{Pa} \times C_\delta \quad (2)$$

$$f_{V_{\div\delta}}(V_{Pa}) = V_{Pa} \div C_\delta \quad (3)$$

These are primarily useful for carrying out kinematics and dynamics calculations.

Time – Current Time Difference Variables The slightly more complex time – current time difference (TCTD) variables $\mathcal{V}_{\Delta T} \subseteq \mathcal{V}$ calculate the duration between the input of the variable and the current time C_T as follows:

$$f_{V_{\Delta T}}(V_{Pa}) = V_{Pa} - C_T \quad (4)$$

TCTD variables are primarily useful within the control modules described in Sec. 6, where they can be utilised to determine the duration of time between now and when a planned action goal should be accomplished by.

Time Conditional Variables Lastly we introduce time conditional variables $\mathcal{V}_{T?} \subseteq \mathcal{V}$ that take the current time C_T and compare it against a predetermined time in order to select which parent from which to derive its output. Their structural equations are defined as follows:

$$f_{V_{T?}}(V_{Pa}^0, V_{Pa}^1) = \begin{cases} V_{Pa}^0 & C_T < \theta_T \\ V_{Pa}^1 & C_T \geq \theta_T \end{cases} \quad (5)$$

where θ_T is a configurable time parameter specified during structural equation construction. Time conditional variables have multiple uses including dynamic addition / subtraction of agents in environment interaction calculations. Furthermore though, they can be utilised for counterfactual simulation purposes, as one can effectively splice together a new counterfactual SCM together with an original SCM. From here θ_T can be used to dictate the divergence point between the original and counterfactual SCM histories.

5.4 Buffer Variables

Having introduced the variable context and explored how one can utilise temporal variables to interact with the meta-variables of \mathcal{C} we can now utilise this to store time-indexed variable data encapsulated within the SCM. Buffer variables $\mathcal{V}_B \subseteq \mathcal{V}$ each have a single parent, i.e. $\forall V_B \in \mathcal{V}_B |Pa(V_B)| = 1$, and as the name suggests they act as a buffer for this parent, storing data relevant to it. In order to do so a buffer variable V_B maintains a time-indexed dictionary $D_{V_B} = \langle \mathcal{T}_{V_B}, d_{V_B} \rangle$ where $\mathcal{T}_{V_B} \subset \mathcal{T}$ is the set of time steps with indexed data, and $d_{V_B}(\cdot) : \mathcal{T} \rightarrow \tau_{V_B}$ is a function that maps a time step to a value or distribution for variable V_B of type τ_{V_B} . With this established we can establish the structural equation for a given buffer variable $f_{V_B} \in \mathcal{F}$ as follows:

$$f_{V_B}(V_{Pa}) = \begin{cases} \text{UP}_{\{\}}(d_{V_B}(C_T)) & C_T \in \mathcal{T}_{V_B} \\ \text{UP}_{\{(D_{V_B}, C_T, V_{Pa})\}}(V_{Pa}) & C_T \notin \mathcal{T}_{V_B} \end{cases} \quad (6)$$

Here $f_{V_B}(\cdot) : \tau_{V_{Pa}} \rightarrow \mathfrak{B}(\tau_{V_{Pa}})$ either returns the output of its parent variable, or retrieves stored data, depending upon whether the current time C_T is found within the dictionary

time steps \mathcal{T}_{V_B} . Importantly the output type of V_B matches that of its parent V_{Pa} , denoted as $\tau_{V_{Pa}}$, albeit with the addition of wrapping the type in the buffer monad \mathfrak{B} . The buffer monad takes a single type and provides a data constructor $\text{UP}_x(\cdot)$ (i.e. update with x). The data constructor takes a set x of tuples structured (D, T, V) and for each tuple stores the output of V at tuple creation within the dictionary D time-indexed to time step $T \in \mathcal{T}$. In order to comply with the requirements for defining a monad, we provide the following unit and bind functions:

$$u_{\mathfrak{B}}(V) = \text{UP}_{\{\}}(V) \quad (7)$$

$$b_{\mathfrak{B}}(\text{UP}_x(V), f) = f(V) \triangleright_{\mathfrak{B}} (\lambda \text{UP}_{x'}(V'). \text{UP}_{x \cup x'}(V')) \quad (8)$$

This monad bears resemblance to the writer monad (Jones and Duponcheel 1993) albeit with the addition of time-indexed writing to the specified buffer variable dictionaries.

5.5 Socket Variables

As mentioned in Sec. 4.1 SCMs are inherently well suited to modularisation (Pearl 2009). Since exogenous variables capture factors outside of the model that nonetheless influence the model, if one then produces a model for these factors they can easily combine the SCMs together to form a new greater whole. The main limitations of the naive combination of SCMs is the lack of ability for system designers to set limits on how SCMs are joined, and the difficulty in dynamically separating SCMs without a means of representing where they are joined.

Thus we decompose the exogenous variables \mathcal{U} into socket variables \mathcal{S} and hidden exogenous variables \mathcal{U}_H . A socket variable $S \in \mathcal{S}$ differs from a typical exogenous variable in that its value is conditionally derived as follows:

$$S \leftarrow \begin{cases} f_S(Pa(S)) & f_S \in \mathcal{F} \\ P(S) & f_S \notin \mathcal{F} \end{cases} \quad (9)$$

where f_S is a structural equation that derives a value for socket variable S . This allows one to join SCMs by assigning S to take the output of a variable from another SCM. Importantly tracking socket variables separately ensures that the act of joining SCMs is reversable, allowing the dynamic reconfiguration of SCM-based modules.

Lastly, the previously described decomposition leaves us with a set of hidden exogenous variables \mathcal{U}_H , which for all intents and purposes are normal exogenous variables. However, it is assumed that access to modify $P(\mathcal{U}_H)$ is determined by system design following principles of encapsulation, hence they are ‘‘hidden’’ behind the SCM wrapper.

5.6 Retrospective Causal Stationarity with Mutable Input Sets

In order to capture a system of multiple agents interacting within a shared environment, it is necessary to be able to support the collation of a dynamic number of sources of input data into a set. The dynamic element is of key importance here, as it is trivial to construct a structural equation which takes input from several agent interactions and either outputs on or operates upon a set, provided the inputs are

known and their number remains fixed. Thus the challenge is extending SCMs to allow the dynamic introduction and removal of SCM modules corresponding to agents entering and leaving the perceived environment.

The issue with this is that altering the structural equations of SCMs amounts to a breach of causal stationarity (Runge 2018), which poses an issue for window graph roll-outs, our own PTS variable temporal representation, as well as many inference techniques applied to SCMs. However, we can demonstrate that online mutation of an input set to a structural equation can be supported while maintaining a form of causal stationarity:

Definition 1 (Retrospective Causal Stationarity). Let \mathcal{T} be defined in such a way that $\min \mathcal{T} = 0$. A fixed SCM \mathcal{M}_T that accurately models causal relations for time $T \in \mathcal{T}$ has retrospective causal stationarity (RCS) if it accurately models all previous time steps $\mathcal{T}_{<T} = \{T' \mid T' < T, T' \in \mathcal{T}\}$. This effectively means that if T is the most recently observed time step, \mathcal{M}_T can be utilised for inference and such without concern for a lack of causal stationarity.

From here we can define a theorem supporting the use of a dynamic set of inputs for a structural equation:

Theorem 1 (Mutable Input Set RCS). *One can capture the dynamic introduction and removal of sources of type $\mathbb{N} \times \tau_X$ used together as an input set for a variable V_Y with structural equation $f_{V_Y}(\cdot) : 2^{\mathbb{N} \times \tau_X} \rightarrow \tau_{V_Y}$ via series of SCMs $\{\mathcal{M}_0, \mathcal{M}_\delta, \dots, \mathcal{M}_T\}$ that each provide retrospective temporal stationarity.*

Here the set of natural numbers \mathbb{N} is used to uniquely identify contributions from different sources (e.g. agents) and importantly allows the same value of type τ_X to be captured several times within the input set.

We first describe the structure utilised within the SCM in order to construct sets from variable outputs. The input to V_Y is incrementally built up from the combination of:

- A socket variable S_\emptyset where the probability distribution $P(S_\emptyset)$ is a degenerate distribution that always returns the empty set \emptyset .
- A union variable V_\cup that has two parents providing input sets of type $2^{\mathbb{N} \times \tau_X}$ and outputs the union of said sets. The first of these parents provides a singleton set from a given source (e.g. an agent), while the second parent is a socket variable as described above.

This effectively allows the system to iteratively construct a set beginning with S_\emptyset providing an empty set. From here one can connect a union variable V_\cup in order to incorporate a new input into the set, while providing its own socket variable S'_\emptyset from which additional another union variable could be connected in future. This structure allows for the dynamic introduction and removal of input sources, as it effectively emulates a linked list.

We can now consider the following basic lemma:

Lemma 1.1 (Base Case). *Provided the SCM \mathcal{M}_0 at the first time step is accurate for said time step, it has retrospectively causal stationarity.*

Proof of Lemma 1.1. Given that \mathcal{M}_0 accurately models causal relations for $T = 0$, and $\mathcal{T}_{<0} = \emptyset$, it automatically follows that \mathcal{M}_0 accurately models time steps in $\mathcal{T}_{<0}$. \square

So that we may capture the dynamic nature of the input set sources, rather than having an input source feed directly into a union variable V_{\cup} , it should instead feed through a pair of time conditional variables $V_{T?}^{\alpha}$ and $V_{T?}^{\omega}$. These variables should only return the input set source for $\theta_T^{\alpha} \leq T \leq \theta_T^{\omega}$ where θ_T^{α} and θ_T^{ω} are configurable time parameters for each of the aforementioned time conditional variables respectively. Should T fall outside of these bounds, the time conditional variables should return the output of a fixed exogenous variable U_{\emptyset} where $P(U_{\emptyset})$ is a degenerate distribution that always returns the empty set \emptyset .

Lemma 1.2 (Introduction Induction Step). *If $\mathcal{M}_{T-\delta}$ is an SCM with RCS and at least one new input set source is introduced at the next time step T then one can construct a new SCM \mathcal{M}_T that accurately captures causal relationships at time step T and has RCS.*

Proof of Lemma 1.2. Construct \mathcal{M}_T by extending the SCM to incorporate the new input set sources as described above, assign $\theta_T^{\alpha} = T$ and $\theta_T^{\omega} = T$ for their time conditional variable parameters. Based upon the configuration described above, $\theta_T^{\alpha} \leq T \leq \theta_T^{\omega}$ and thus \mathcal{M}_T will include the new input set source, accurately reflecting the causal relations at time T .

Meanwhile, given that $\mathcal{T}_{<T}$ is defined as all time steps less than T , and now $\theta_T^{\alpha} = T$, we can conclude that for all previous time steps captured by $\mathcal{T}_{<T}$, the new SCM extension will only contribute \emptyset to the input set. This effectively emulates the input set source not being present in the past, accurately reflecting the causal relationships present during those time steps. As such, we can conclude that \mathcal{M}_T also has RCS following the introduction of new input set sources. \square

Lemma 1.3 (Status Quo / Removal Induction Step). *If $\mathcal{M}_{T-\delta}$ is an SCM with RCS and zero or more input set sources are removed at the next time step T then one can construct a new SCM \mathcal{M}_T that accurately captures causal relationships at time step T and has RCS.*

Proof of Lemma 1.3. At each time step T , for each input set source that is present in the modelled system, assign $\theta_T^{\omega} = T$ for the configurable parameter of the associated $V_{T?}^{\omega}$ in \mathcal{M}_T respectively. SCM input set sources for which $\theta_T^{\alpha} \leq T \leq \theta_T^{\omega}$ have their contributions included in the input set. Thus, this update combined with Lemma 1.2 ensures that all input set sources that are present in the modelled system will have their contributions captured within the input set, as is accurate for time step T .

All the while, θ_T^{α} is always first initialised to the time step in which the associated input set source was introduced — as per Proof of Lemma 1.2 — and is only updated as described above. As such, if an update is missed for a given input set source — i.e. due to it no longer being present in the modelled system — then it follows that $T > \theta_T^{\alpha}$, and thus the SCM input set source will return \emptyset , no longer contributing to the input set. In doing so the SCM remains accurate for

time step T , and additionally retains the same behaviour it possessed for previous time steps as θ_T^{α} and θ_T^{ω} remain the same as in $\mathcal{M}_{T-\delta}$. Thus, we can conclude that \mathcal{M}_T also has RCS for instances where the status quo is maintained, and for instances where one or more input set sources are removed. \square

Proof of Theorem 1. We have demonstrated through Lemma 1.1 that the accurate SCM associated with the first time step \mathcal{M}_T automatically has retrospective temporal stationarity, effectively establishing a base case. Additionally we have shown that input set source introductions (Lemma 1.2), removals (Lemma 1.3), or maintaining the status quo of input set sources between time steps (Lemma 1.3) can be done while maintaining RCS for \mathcal{M}_T given that $\mathcal{M}_{T-\delta}$ had it. Thus via induction we can infer that the sequence of SCMs $\{\mathcal{M}_0, \mathcal{M}_{\delta}, \dots, \mathcal{M}_T\}$ accurately captures these dynamic mutations and all possess RCS. \square

6 Case Studies

In order to demonstrate the extensions we have introduced, and as part of the code appendix, we provide two AES architectures developed for the autonomous driving and service robotics domains as case studies. Given that these architectures are comprised of several SCM modules and even a single of these modules requires substantial documentation we have opted to provide a high-level overview of the designs and goals of the architectures here. However, we provide comprehensive documentation of all SCM module specifications in Appendix A of the technical appendix.

Both case studies represent individual AES agents via a planner object to provide high-level goals, a controller to translate those goals into continuous actuation values, and an object representing the embodied system that takes the actuation values as input. The embodied system representation object is further connected to an entity object that represents the embodied system within an environment shared with other agents. These entity objects in turn store a number of link objects that each capture interactions between the entity embodied system and another embodied system.

6.1 Autonomous Driving

Our primary motivation behind developing an SCM architecture capturing the interactions of AESs in autonomous driving scenarios is for post-hoc analysis of scenarios. Critically, driving presents a safety critical domain that nonetheless presents a greater degree of order in terms of the expectation that road agents follow the laws of the road. The combination of these traits makes it both appealing and convenient to model causally.

An overview of the autonomous driving SCM architecture is depicted in Fig. 2a. Within this domain, we have formulated AES goals as a combination of a target lane and a target speed with corresponding times by which to achieve these goals. These goals are converted into motor torque and steering actuation values via a proportional feedback controller. The motor torque and steering values are then fed into a dynamic bicycle model (Guiggiani 2018). Meanwhile the entity objects and their associated link objects are used

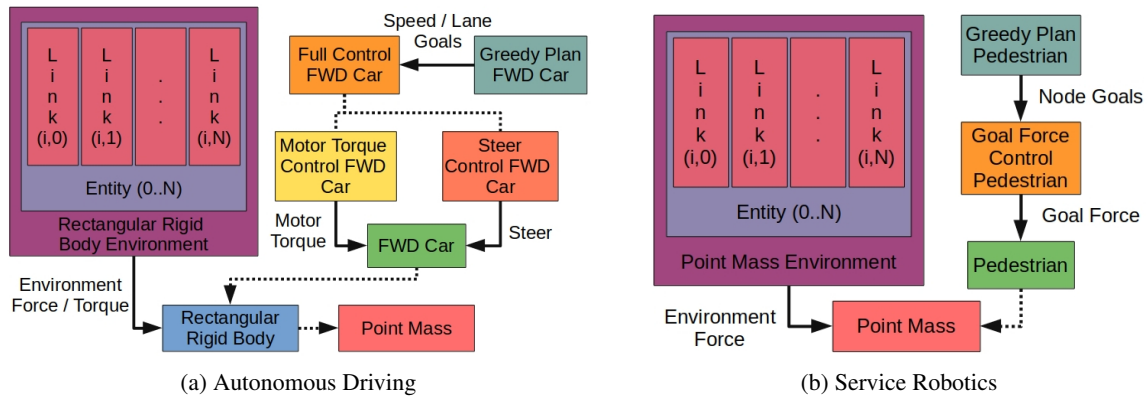


Figure 2: An overview of the architecture of the case study architectures. Solid and dotted lines represent composition and inheritance relationships respectively.

to provide agent collision and drag forces / torques, treating vehicles as rectangular rigid bodies.

6.2 Service Robotics

In contrast to the autonomous driving domain the service robotics domain tends to carry substantially less risk. Yet this comes with a significantly greater level of chaos resulting from the free-form nature of action and interaction within pedestrian environments. While this arguably makes modelling such a system that much harder, it also gives us greater motivation to utilise causality in order to try and make sense of the chaos, and because the domain carries less risk, one can utilise such information proactively.

An overview of the service robotics SCM architecture is depicted in Fig. 2b. Since this domain does not have a direct analogue to lanes, the architecture specifies goals in terms of target nodes from a generated graphical road-map and the times by which these nodes should be reached. Given these nodes represent fixed points rather than channels of movement, and the maximum speed of pedestrians is comparatively low, it is also unnecessary to represent speed as a goal separate from the nodes, simplifying the goal representation. The controller once again utilises a simple proportional feedback approach in order to provide a goal force which is applied to a point mass representation of a human / robot. The environment entity and link objects are then used to represent the repulsive forces between agents that mimic the desire for personal space. The goal and repulsion forces combine to approximate the social forces model developed by Helbing & Molnár (1995).

7 Discussion & Future Work

Having now discussed the challenges facing integration of SCMs within AESs, described extensions that help address these challenges, and presented two case studies utilising these extensions, we can now consider how future research could utilise these advances. Our primary motivation in developing this architecture was in advancing the capabilities of XAI for AESs. We took inspiration from the work of Howard & Kunze (2023a) who presented a theory of mind

based approach to discovering high-level causal links between road agents. However, despite the promising results of this work, their methodology was not based upon the use of SCMs, in doing so limiting the range of potential counterfactual queries that could be made.

For example the field of algorithmic recourse (Karimi et al. 2022) has substantial overlap with causal modelling so one could likely integrate such methodologies without much difficulty. Algorithmic recourse pertains to the use of explanation techniques — typically contrastive explanation — in order to bolster the future performance of an agent. Typically these methods have been applied to domains that do not consider embodied systems, making any such work mutually beneficial to both fields.

Despite XAI being a primary driving factor of our work, another key motivator for utilising causality over other XAI techniques was its role in supporting an understanding of behavioural interactions between agents. By considering how the actions of agents can affect the perceived utility and reactions of other agents, AESs can be built to behave more socially acceptable (Rossi, Rossi, and Dautenhahn 2020).

In any case it is clear that most future work will correspond to the use of these extensions within applications. However there is still the opportunity to extend this work at a theoretical level further. The best immediate candidate would be to combine this work, with the MDP-SCM hybrids utilised by other works in causality (Nashed et al. 2023; Cannizzaro and Kunze 2023; Triantafyllou and Radanovic 2023). This would in turn open up further avenues for integration with MDP-based planning research.

To summarise, the presented extensions represent a step forward for both the expressive capabilities of SCMs within causality research as well as work integrating AESs with causality. Through this work, we hope to spur new works bridging the gap between causal reasoning and AES domains such as service robotics, autonomous driving, drone surveying, and beyond. In building such systems we continue the push towards autonomous systems that are transparent, accountable, and understandable. Through these traits we can best ensure that the technologies of tomorrow are developed responsibly.

References

- Adadi, A.; and Berrada, M. 2018. Peeking Inside the Black-Box: A Survey on Explainable Artificial Intelligence (XAI). *IEEE Access*, 6: 52138–52160.
- Bareinboim, E.; Forney, A.; and Pearl, J. 2015. Bandits with Unobserved Confounders: A Causal Approach. In Cortes, C.; Lawrence, N.; Lee, D.; Sugiyama, M.; and Garnett, R., eds., *Advances in Neural Information Processing Systems*, volume 28. Curran Associates, Inc.
- Bongers, S.; Forré, P.; Peters, J.; and Mooij, J. M. 2021. Foundations of structural causal models with cycles and latent variables. *The Annals of Statistics*, 49(5): 2885–2915.
- Cannizzaro, R.; and Kunze, L. 2023. CAR-DESPOT: Causally-Informed Online POMDP Planning for Robots in Confounded Environments. In *2023 IEEE/RSJ International Conference on Intelligent Robots and Systems (IROS)*, 2018–2025.
- Castri, L.; Mghames, S.; Hanheide, M.; and Bellotto, N. 2022. Causal Discovery of Dynamic Models for Predicting Human Spatial Interactions. In Cavallo, F.; Cabibihan, J.-J.; Fiorini, L.; Sorrentino, A.; He, H.; Liu, X.; Matsumoto, Y.; and Ge, S. S., eds., *Social Robotics*, 154–164. Cham: Springer Nature Switzerland. ISBN 978-3-031-24667-8.
- Dennett, D. C. 1971. Intentional Systems. *The Journal of Philosophy*, 68(4): 87–106.
- Diehl, M.; and Ramirez-Amaro, K. 2023. A causal-based approach to explain, predict and prevent failures in robotic tasks. *Robotics and Autonomous Systems*, 162: 104376.
- Gadd, M.; de Martini, D.; Marchegiani, L.; Newman, P.; and Kunze, L. 2020. Sense-Assess-eXplain (SAX): Building Trust in Autonomous Vehicles in Challenging Real-World Driving Scenarios. In *2020 IEEE Intelligent Vehicles Symposium (IV)*, 150–155.
- Gerstenberg, T. 2022. What would have happened? Counterfactuals, hypotheticals and causal judgements. *Philosophical Transactions of the Royal Society B*, 377(1866): 20210339.
- Granger, C. W. J. 1969. Investigating Causal Relations by Econometric Models and Cross-spectral Methods. *Econometrica*, 37(3): 424–438.
- Guiggiani, M. 2018. *The Science of Vehicle Dynamics: Handling, Braking, and Ride of Road and Race Cars*. Springer.
- Gunning, D.; and Aha, D. 2019. DARPA’s Explainable Artificial Intelligence (XAI) Program. *AI Magazine*, 40(2): 44–58.
- Gyevnar, B.; Wang, C.; Lucas, C. G.; Cohen, S. B.; and Albrecht, S. V. 2024. Causal Explanations for Sequential Decision-Making in Multi-Agent Systems. In *Proceedings of the 23rd International Conference on Autonomous Agents and Multiagent Systems, AAMAS ’24*, 771–779. Richland, SC: International Foundation for Autonomous Agents and Multiagent Systems. ISBN 9798400704864.
- Helbing, D.; and Molnár, P. 1995. Social force model for pedestrian dynamics. *Phys. Rev. E*, 51: 4282–4286.
- Hellström, T. 2021. The relevance of causation in robotics: A review, categorization, and analysis. *Paladyn, Journal of Behavioral Robotics*, 12(1): 238–255.
- Howard, R.; and Kunze, L. 2023a. Simulation-Based Counterfactual Causal Discovery on Real World Driver Behaviour. In *2023 IEEE Intelligent Vehicles Symposium (IV)*, 1–8.
- Howard, R. P. M.; and Kunze, L. 2023b. Evaluating Temporal Observation-Based Causal Discovery Techniques Applied to Road Driver Behaviour. In van der Schaar, M.; Zhang, C.; and Janzing, D., eds., *Proceedings of the Second Conference on Causal Learning and Reasoning*, volume 213 of *Proceedings of Machine Learning Research*, 473–498. PMLR.
- Jones, M. P.; and Duponcheel, L. 1993. Composing monads. Technical Report YALEU/DCS/RR-1004, Department of Computer Science. Yale University.
- Karimi, A.-H.; Barthe, G.; Schölkopf, B.; and Valera, I. 2022. A Survey of Algorithmic Recourse: Contrastive Explanations and Consequential Recommendations. *ACM Comput. Surv.*, 55(5).
- Macenski, S.; Foote, T.; Gerkey, B.; Lalancette, C.; and Woodall, W. 2022. Robot Operating System 2: Design, architecture, and uses in the wild. *Science Robotics*, 7(66): eabm6074.
- Madumal, P.; Miller, T.; Sonenberg, L.; and Vetere, F. 2020. Explainable Reinforcement Learning through a Causal Lens. *Proceedings of the AAAI Conference on Artificial Intelligence*, 34(03): 2493–2500.
- Maier, R.; Grabinger, L.; Urlhart, D.; and Mottok, J. 2024. Causal Models to Support Scenario-Based Testing of ADAS. *IEEE Transactions on Intelligent Transportation Systems*, 25(2): 1815–1831.
- Marfil, R.; Bustos, P.; and Bandera, A. 2024. Causal-Based Approaches to Explain and Learn from Self-Extension—A Review. *Electronics*, 13(7).
- Mooij, J. M.; Janzing, D.; and Schölkopf, B. 2013. From ordinary differential equations to structural causal models: the deterministic case. In *Proceedings of the Twenty-Ninth Conference on Uncertainty in Artificial Intelligence, UAI’13*, 440–448. Arlington, Virginia, USA: AUAI Press.
- Nashed, S. B.; Mahmud, S.; Goldman, C. V.; and Zilberstein, S. 2023. Causal Explanations for Sequential Decision Making Under Uncertainty. In *Proceedings of the 2023 International Conference on Autonomous Agents and Multiagent Systems, AAMAS ’23*, 2307–2309. Richland, SC: International Foundation for Autonomous Agents and Multiagent Systems. ISBN 9781450394321.
- Nauta, M.; Bucur, D.; and Seifert, C. 2019. Causal Discovery with Attention-Based Convolutional Neural Networks. *Machine Learning and Knowledge Extraction*, 1(1): 312–340.
- Pearl, J. 2009. *Causality*. Cambridge university press.
- Peters, J.; Janzing, D.; and Schölkopf, B. 2017. *Elements of causal inference: foundations and learning algorithms*, chapter 10. The MIT Press.

- Poehhacker, N.; and Kacianka, S. 2021. Algorithmic Accountability in Context. Socio-Technical Perspectives on Structural Causal Models. *Frontiers in Big Data*, 3.
- Rossi, S.; Rossi, A.; and Dautenhahn, K. 2020. The secret life of robots: perspectives and challenges for robot's behaviours during non-interactive tasks. *International Journal of Social Robotics*, 12(6): 1265–1278.
- Runge, J. 2018. Causal network reconstruction from time series: From theoretical assumptions to practical estimation. *Chaos: An Interdisciplinary Journal of Nonlinear Science*, 28(7): 075310.
- Salmon, W. C. 1998. *Causality and explanation*. Oxford University Press.
- Scott, M. L. 2009. *Programming Language Pragmatics, Third Edition*. San Francisco, CA, USA: Morgan Kaufmann Publishers Inc., 3rd edition. ISBN 0123745144.
- Triantafyllou, S.; and Radanovic, G. 2023. Towards Computationally Efficient Responsibility Attribution in Decentralized Partially Observable MDPs. In *Proceedings of the 2023 International Conference on Autonomous Agents and Multiagent Systems, AAMAS '23*, 131–139. Richland, SC: International Foundation for Autonomous Agents and Multiagent Systems. ISBN 9781450394321.
- von Eschenbach, W. J. 2021. Transparency and the black box problem: Why we do not trust AI. *Philosophy & Technology*, 34(4): 1607–1622.
- Wadler, P. 1992. The essence of functional programming. In *Proceedings of the 19th ACM SIGPLAN-SIGACT symposium on Principles of programming languages*, 1–14.
- Wich, A.; Schultheis, H.; and Beetz, M. 2022. Empirical Estimates on Hand Manipulation are Recoverable: A Step Towards Individualized and Explainable Robotic Support in Everyday Activities. In *Proceedings of the 21st International Conference on Autonomous Agents and Multiagent Systems, AAMAS '22*, 1382–1390. Richland, SC: International Foundation for Autonomous Agents and Multiagent Systems. ISBN 9781450392136.
- Yang, M.; Liu, F.; Chen, Z.; Shen, X.; Hao, J.; and Wang, J. 2021. CausalVAE: Disentangled Representation Learning via Neural Structural Causal Models. In *Proceedings of the IEEE/CVF Conference on Computer Vision and Pattern Recognition (CVPR)*, 9593–9602.

Extending Structural Causal Models for Autonomous Embodied Systems — Technical Appendix

Rhys P. M. Howard¹, Lars Kunze²,

¹Oxford Robotics Institute, Dept. of Eng. Sci., University of Oxford, 17 Parks Road, Oxford, OX1 3PJ, UK

²Bristol Robotics Laboratory, T-Block, UWE Bristol, Bristol, BS16 1QY, UK

rhyshoward@live.com, lars.kunze@uwe.ac.uk

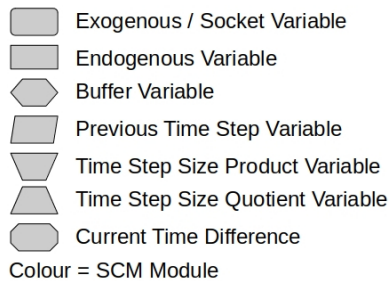


Figure 1: SCM Legend

A Detailed SCM Specification

Before describing the various SCMs of the case study architectures, it is beneficial to describe the format that will be used here. Each subsection will be comprised of the following components:

- A textual description of the purpose of the SCM, and its relation to other SCMs.
- A figure illustrating the graphical layout of the SCM. A legend for the SCM figures is given in Fig. 1.
- A list of the variables and their associated structural equations / distributions. These are further defined as endogenous, hidden exogenous, and socket variables. Structural equations will either be explicitly defined for simple equations, or described textually for more complex equations. Some variable distributions are specified to be initialisation parameters, as these are not predefined, but set at the time of SCM construction. For simplicity's sake, monads will be omitted from data type specification.

For a recapitulation of the overall case study architectures see Fig. 2 and Fig. 3 for the autonomous driving and service robotics case study SCM architectures respectively.

A.1 Point Mass

Description As the name suggests, represents a 2D dynamic point mass (Blum and Lototsky 2006) that does not explicitly occupy any portion of space yet provides the represented object with a mass, position, linear velocity, linear acceleration, and input forces which influence these. This

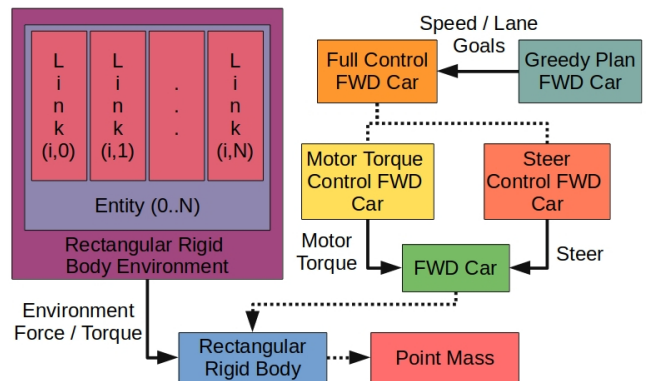


Figure 2: Autonomous Driving SCM Architecture

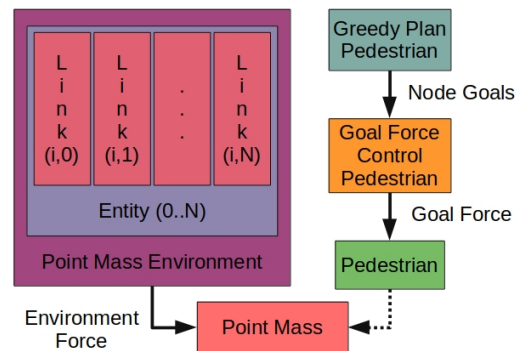


Figure 3: Service Robotics SCM Architecture

SCM effectively provides the base physical representation of an agent within both architectures.

Graphical Layout Fig. 4 illustrates the graphical layout of the *Point Mass* SCM.

Variables

Hidden Exogenous:

- *id*
 - Description: Unique identifier for the point mass.
 - Data Type: \mathbb{Z}
 - Distribution: $\langle \text{initialisation parameter} \rangle$

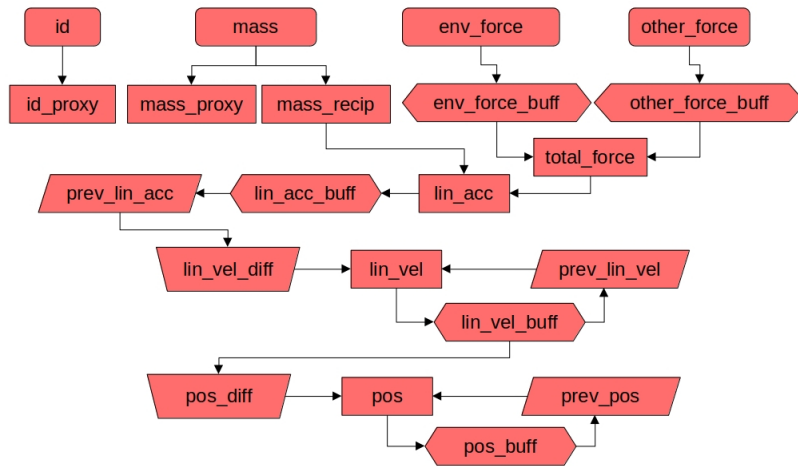


Figure 4: *Point Mass* SCM

- *mass*

- Description: Mass of the point mass object.
- Data Type: \mathbb{R}
- Distribution: $\langle \text{initialisation parameter} \rangle$

Socket:

- *env_force*

- Description: Total forces from the environment affecting the point mass object.
- Data Type: \mathbb{R}^2
- Default Distribution: $Degenerate([0, 0]^\top)$

- *other_force*

- Description: Total forces from sources other than the shared environment (e.g. a super class, a controller).
- Data Type: \mathbb{R}^2
- Default Distribution: $Degenerate([0, 0]^\top)$

Endogenous:

- *id_proxy*

- Description: Proxy for the *id* variable.
- Data Type: \mathbb{Z}
- Structural Equation: *id*

- *mass_proxy*

- Description: Proxy for the *mass* variable.
- Data Type: \mathbb{R}
- Structural Equation: *mass*

- *mass_recip*

- Description: Reciprocal of the *mass* variable.
- Data Type: \mathbb{R}
- Structural Equation: $mass^{-1}$

- *env_force_buff*

- Description: Buffer for the *env_force* variable.
- Data Type: \mathbb{R}^2

- Structural Equation: $f_{V_B}(env_force)$

- *other_force_buff*

- Description: Buffer for the *other_force* variable.
- Data Type: \mathbb{R}^2
- Structural Equation: $f_{V_B}(other_force)$

- *total_force*

- Description: Combines the *env_force* and *other_force* variables through addition.
- Data Type: \mathbb{R}^2
- Structural Equation: $env_force + other_force$

- *lin_acc*

- Description: Linear acceleration determined via *total_force* and *mass_recip* variables.
- Data Type: \mathbb{R}^2
- Structural Equation: $total_force \times mass_recip$

- *lin_acc_buff*

- Description: Buffer for the *lin_acc* variable.
- Data Type: \mathbb{R}^2
- Structural Equation: $f_{V_B}(lin_acc)$

- *prev_lin_acc*

- Description: Represents the *lin_acc* variable for the previous time step via the *lin_acc_buff* variable.
- Data Type: \mathbb{R}^2
- Structural Equation: $f_{V_\delta}(lin_acc_buff)$

- *lin_vel_diff*

- Description: Linear velocity difference calculated based upon the *prev_lin_acc* variable. Note that *prev_lin_acc* has to be used over *lin_acc_buff* to avoid a cycle within the SCM.

- Data Type: \mathbb{R}^2

- Structural Equation: $f_{V_{\times\delta}}(prev_lin_acc)$

- *prev_lin_vel*

- Description: Represents the lin_vel variable for the previous time step via the lin_vel_buff variable.
- Data Type: \mathbb{R}^2
- Structural Equation: $f_{V_\delta}(lin_vel_buff)$
- lin_vel
 - Description: Linear velocity determined via $prev_lin_vel$ and lin_vel_diff variables.
 - Data Type: \mathbb{R}^2
 - Structural Equation: $prev_lin_vel + lin_vel_diff$
- lin_vel_buff
 - Description: Buffer for the lin_vel variable.
 - Data Type: \mathbb{R}^2
 - Structural Equation: $f_{V_B}(lin_vel)$
- pos_diff
 - Description: Position difference calculated based upon the lin_vel_buff variable.
 - Data Type: \mathbb{R}^2
 - Structural Equation: $f_{V_\delta}(lin_vel_buff)$
- $prev_pos$
 - Description: Represents the pos variable for the previous time step via the pos_buff variable.
 - Data Type: \mathbb{R}^2
 - Structural Equation: $f_{V_\delta}(pos_buff)$
- pos
 - Description: Position determined via $prev_pos$ and pos_diff variables.
 - Data Type: \mathbb{R}^2
 - Structural Equation: $prev_pos + pos_diff$
- pos_buff
 - Description: Buffer for the pos variable.
 - Data Type: \mathbb{R}^2
 - Structural Equation: $f_{V_B}(pos)$

A.2 Point Mass Entity

Description Specific to the service robotics architecture, this provides a representation of a point mass within a shared environment. Because this is tailored to the service robotics domain this amounts to a sum of avoidance forces provided by the *Point Mass Link* SCMs associated with a given *Point Mass Entity* SCM.

Graphical Layout Fig. 5 illustrates the graphical layout of the *Point Mass Entity* SCM. Note this SCM is extremely simple, only comprising a single variable, however we have nonetheless provided an illustration for completeness.

Variables

Endogenous:

- env_force
 - Description: Sums the repulsive forces contributed by *Point Mass Link* SCMs associated with this SCM.
 - Data Type: \mathbb{R}^2
 - Structural Equation: $\sum_{i=1}^{|links|} actual_avoidance_force_i$

A.3 Point Mass Link

Description Captures the interactions between two point masses in a shared environment. Again because this is tailored to a service robotics scenario, these links capture avoidance forces in line with a social forces model (Helbing and Molnár 1995), with the repulsive forces scaling inversely to the exponent of the distance between the point masses. Variables belonging to the primary and secondary *Point Mass* SCMs associated with the link will be indicated via A and B subscripts respectively.

Graphical Layout Fig. 6 illustrates the graphical layout of the *Point Mass Link* SCM¹.

Variables

Hidden Exogenous:

- $dist_scale_factor$
 - Description: Scale factor for the repulsive force captured by the link.
 - Data Type: \mathbb{R}
 - Distribution: *Degenerate*(1)

Endogenous:

- neg_other_pos
 - Description: Negation of the pos_B variable from the secondary *Point Mass* SCM of the link.
 - Data Type: \mathbb{R}^2
 - Structural Equation: $-pos_B$
- pos_diff
 - Description: Vector from the secondary *Point Mass* SCM pos_B variable to the primary *Point Mass* SCM pos_buff_A variable calculated via summing the pos_buff_A and neg_other_pos variables.
 - Data Type: \mathbb{R}^2
 - Structural Equation: $pos_buff_A + neg_other_pos$
- $dist$
 - Description: Calculates the norm of the pos_diff variable.
 - Data Type: \mathbb{R}
 - Structural Equation: $\|pos_diff\|$
- $scaled_dist$
 - Description: Scales the $dist$ variable by the $dist_scale_factor$ variable.
 - Data Type: \mathbb{R}
 - Structural Equation: $dist \times dist_scale_factor$
- neg_scaled_dist
 - Description: Negation of the $scaled_dist$ variable.
 - Data Type: \mathbb{R}
 - Structural Equation: $-scaled_dist$

¹The colouring of the SCM graph illustrations will be updated such that the *Point Mass* and *Point Mass Link* SCMs do not use the same colouring in the camera-ready version.

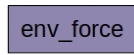


Figure 5: Point Mass Entity SCM

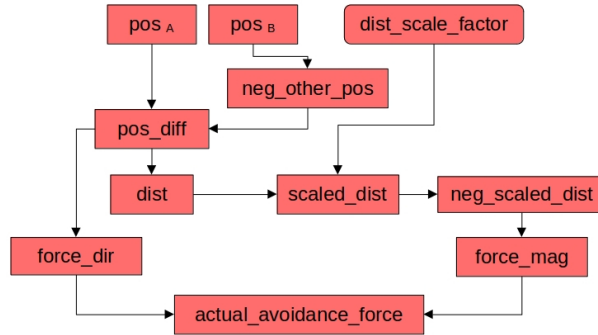


Figure 6: Point Mass Link SCM

- *force_mag*
 - Description: Calculates the exponential function of the *neg_scaled_dist* variable.
 - Data Type: \mathbb{R}
 - Structural Equation: $e^{neg_scaled_dist}$
- *force_dir*
 - Description: Normalisation of the *pos_diff* variable.
 - Data Type: \mathbb{R}^2
 - Structural Equation: $pos_diff \times ||pos_diff||^{-1}$
- *actual_avoidance_force*
 - Description: Repulsive force for the link calculated by multiplying the *force_dir* and *force_mag* variables.
 - Data Type: \mathbb{R}^2
 - Structural Equation: $force_dir \times force_mag$

A.4 Rectangular Rigid Body

Description Inherits from the *Point Mass* SCM, extending it to represent a 2D rectangular rigid body (Blum and Lototsky 2006). In doing so it allows the object to occupy a rectangular portion of space and provides it with a moment of inertia, rotation, angular velocity, angular acceleration, and input torques which influence these. This SCM was primarily created with use in the autonomous driving architecture as collisions and their consequences are of far greater importance to capture in safety critical driving scenarios, not to mention that a vehicle’s orientation has far greater sway over its motion than with a pedestrian. This SCM additionally tracks the open space in-front of the rectangular rigid body, as this information is calculated via the *Rectangular Rigid Body Entity* SCM via which a rectangular rigid body is represented in a shared environment.

Graphical Layout Fig. 7 illustrates the graphical layout of the *Rectangular Rigid Body* SCM.

Variables

Hidden Exogenous:

- *length*
 - Description: Length of the rectangular rigid body.
 - Data Type: \mathbb{R}
 - Distribution: $\langle \text{initialisation parameter} \rangle$
- *width*
 - Description: Width of the rectangular rigid body.
 - Data Type: \mathbb{R}
 - Distribution: $\langle \text{initialisation parameter} \rangle$
- *height*
 - Description: Height of the rectangular rigid body. Note that since the dynamics calculations only capture 2D physics, this variable is mostly supplementary.
 - Data Type: \mathbb{R}
 - Distribution: $\langle \text{initialisation parameter} \rangle$
- *drag_area*
 - Description: The drag area of the rectangular rigid body as a 3D object. Allows drag calculations despite the dynamics being restricted to a 2D plane.
 - Data Type: \mathbb{R}
 - Distribution: $\langle \text{initialisation parameter} \rangle$
- *moi_scale_factor*
 - Description: Provides the $\frac{1}{12}$ scale factor for calculating moment of inertia of a rectangular around the Z / vertical axis.
 - Data Type: \mathbb{R}
 - Distribution: $Degenerate(0.0833)$

Socket:

- *dist_headway*
 - Description: The empty space in-front of the rectangular rigid body. This typically receives input from a *Rectangular Rigid Body Entity* SCM representing the

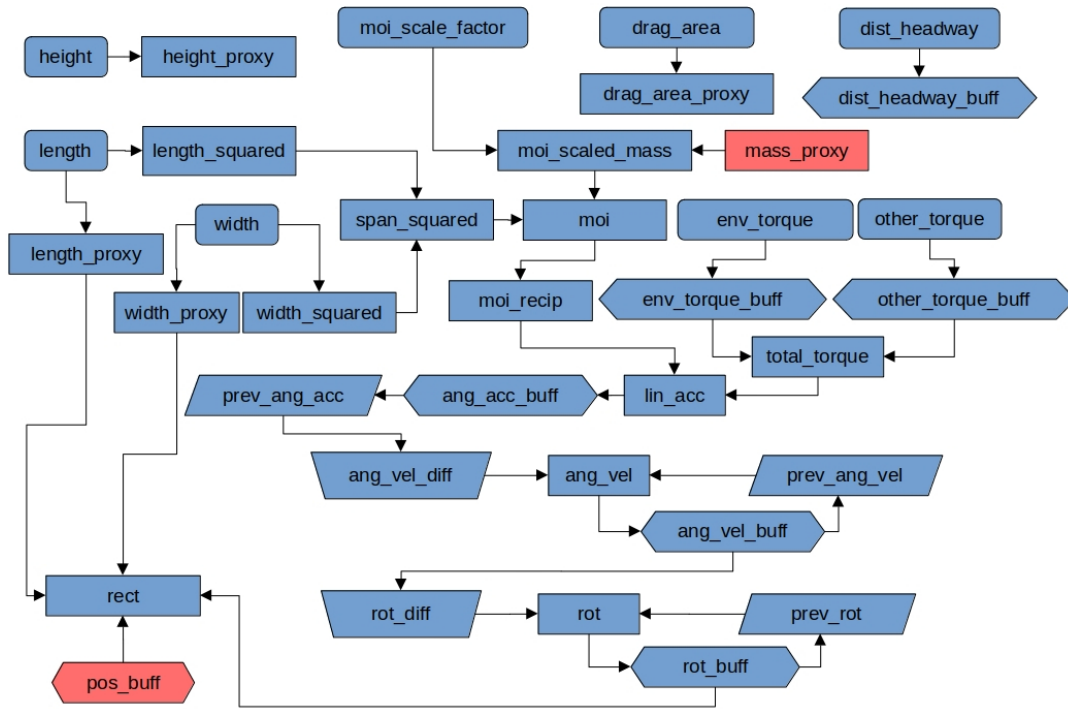


Figure 7: Rectangular Rigid Body SCM

Rectangular Rigid Body SCM within a shared environment, and is primarily utilised within the context of the autonomous driving architecture as a safety metric.

- Data Type: \mathbb{R}
- Default Distribution: *Degenerate*(100)
- *env_torque*
 - Description: Total torques from the environment affecting the rectangular rigid body object.
 - Data Type: \mathbb{R}
 - Default Distribution: *Degenerate*(0)
- *other_torque*
 - Description: Total torques from sources other than the shared environment (e.g. a super class, a controller).
 - Data Type: \mathbb{R}
 - Default Distribution: *Degenerate*(0)

Endogenous:

- *length_proxy*
 - Description: Proxy for the *length* variable.
 - Data Type: \mathbb{R}
 - Structural Equation: *length*
- *length_squared*
 - Description: Square of the *length* variable.
 - Data Type: \mathbb{R}
 - Structural Equation: *length* \times *length_proxy*
- *width_proxy*

- Description: Proxy for the *width* variable.
- Data Type: \mathbb{R}
- Structural Equation: *width*
- *width_squared*
 - Description: Square of the *width* variable.
 - Data Type: \mathbb{R}
 - Structural Equation: *width* \times *width_proxy*
- *height_proxy*
 - Description: Proxy for the *width* variable.
 - Data Type: \mathbb{R}
 - Structural Equation: *width*
- *drag_area_proxy*
 - Description: Proxy for the *drag_area* variable.
 - Data Type: \mathbb{R}
 - Structural Equation: *drag_area*
- *moi_scaled_mass*
 - Description: Scales the *mass_proxy* variable by *moi_scale_factor*. The first step in calculating the moment of inertia for the rectangular rigid body.
 - Data Type: \mathbb{R}
 - Structural Equation: *drag_area*
- *span_squared*
 - Description: Calculates the square of the span of the rectangular rigid body via Pythagoras theorem together with the *length_squared* and *width_squared* variables.

- Data Type: \mathbb{R}
- Structural Equation: $length_squared + width_squared$
- *moi*
 - Description: The moment of inertia of the rectangular rigid body, calculate via multiplying the *moi_scaled_mass* and *span_squared* variables.
 - Data Type: \mathbb{R}
 - Structural Equation: $moi_scaled_mass \times span_squared$
- *moi_recip*
 - Description: Reciprocal of the *moi* variable.
 - Data Type: \mathbb{R}
 - Structural Equation: moi^{-1}
- *dist_headway_buff*
 - Description: Buffer for the *dist_headway* variable.
 - Data Type: \mathbb{R}
 - Structural Equation: $f_{V_B}(dist_headway)$
- *env_torque_buff*
 - Description: Buffer for the *env_torque* variable.
 - Data Type: \mathbb{R}
 - Structural Equation: $f_{V_B}(env_torque)$
- *other_torque_buff*
 - Description: Buffer for the *other_torque* variable.
 - Data Type: \mathbb{R}
 - Structural Equation: $f_{V_B}(other_torque)$
- *total_torque*
 - Description: Combines the *env_torque* and *other_torque* variables through addition.
 - Data Type: \mathbb{R}
 - Structural Equation: $env_torque + other_torque$
- *ang_acc*
 - Description: Angular acceleration determined via *total_torque* and *moi_recip* variables.
 - Data Type: \mathbb{R}
 - Structural Equation: $total_torque \times moi_recip$
- *ang_acc_buff*
 - Description: Buffer for the *ang_acc* variable.
 - Data Type: \mathbb{R}
 - Structural Equation: $f_{V_B}(ang_acc)$
- *prev_ang_acc*
 - Description: Represents the *ang_acc* variable for the previous time step via the *ang_acc_buff* variable.
 - Data Type: \mathbb{R}
 - Structural Equation: $f_{V_\delta}(ang_acc_buff)$
- *ang_vel_diff*
 - Description: Angular velocity difference calculated based upon the *prev_ang_acc* variable. Note that *prev_ang_acc* has to be used over *ang_acc_buff* to avoid a cycle within the SCM.
- Data Type: \mathbb{R}
- Structural Equation: $f_{V_\delta}(prev_ang_acc)$
- *prev_ang_vel*
 - Description: Represents the *ang_vel* variable for the previous time step via the *ang_vel_buff* variable.
 - Data Type: \mathbb{R}
 - Structural Equation: $f_{V_\delta}(ang_vel_buff)$
- *ang_vel*
 - Description: Angular velocity determined via *prev_ang_vel* and *ang_vel_diff* variables.
 - Data Type: \mathbb{R}
 - Structural Equation: $prev_ang_vel + ang_vel_diff$
- *ang_vel_buff*
 - Description: Buffer for the *ang_vel* variable.
 - Data Type: \mathbb{R}
 - Structural Equation: $f_{V_B}(ang_vel)$
- *rot_diff*
 - Description: Rotation difference calculated based upon the *ang_vel_buff* variable.
 - Data Type: \mathbb{R}
 - Structural Equation: $f_{V_\delta}(ang_vel_buff)$
- *prev_rot*
 - Description: Represents the *rot* variable for the previous time step via the *rot_buff* variable.
 - Data Type: \mathbb{R}
 - Structural Equation: $f_{V_\delta}(rot_buff)$
- *rot*
 - Description: Rotation determined via *prev_rot* and *rot_diff* variables.
 - Data Type: \mathbb{R}
 - Structural Equation: $prev_rot + rot_diff$
- *rot_buff*
 - Description: Buffer for the *rot* variable.
 - Data Type: \mathbb{R}
 - Structural Equation: $f_{V_B}(rot)$
- *rect*
 - Description: Rectangle object formed from *pos_buff*, *rot_buff*, *length_proxy*, and *width_proxy* variables.
 - Data Type: Rect
 - Structural Equation: $Rect(pos_buff, rot_buff, length_proxy, width_proxy)$

A.5 Rectangular Rigid Body Entity

Description Represents rectangular rigid body objects within a shared environment. Performs two functions. The first is to calculate environmental forces, combining drag force and the collision forces calculated by the *Rectangular Rigid Body Link* SCMs associated with a given *Rectangular Rigid Body Entity* SCM. The second is to calculate the minimum distance headway given by the aforementioned *Rectangular Rigid Body Link* SCMs in order to determine the

overall distance headway. Variables belonging to the *Rectangular Rigid Body* SCM associated with the link will be indicated via an A subscript.

Graphical Layout Fig. 8 illustrates the graphical layout of the *Rectangular Rigid Entity Body* SCM.

Variables

Hidden Exogenous:

- *half_scale_factor*
 - Description: Scale factor used to half a variable.
 - Data Type: \mathbb{R}
 - Distribution: *Degenerate*(0.5)
- *dist_headway_limit*
 - Description: Limit on the maximum possible distance headway. Effectively the default assuming there are no rectangular rigid bodies in front of the rectangular rigid body represented by the entity.
 - Data Type: \mathbb{R}
 - Distribution: *Degenerate*(100)
- *air_mass_density*
 - Description: The mass density of air, utilised in drag calculations.
 - Data Type: \mathbb{R}
 - Distribution: *Degenerate*(1.2578)
- *drag_torque*
 - Description: A hard coded value of zero for torque from drag. This is certainly not accurate to physics but is sufficient for the purposes of lightweight simulation.
 - Data Type: \mathbb{R}
 - Distribution: *Degenerate*(0)

Endogenous:

- *half_scale_factor_proxy*
 - Description: Proxy for the *half_scale_factor* variable.
 - Data Type: \mathbb{R}
 - Structural Equation: *half_scale_factor*
- *dist_headway_limit_proxy*
 - Description: Proxy for the *dist_headway_limit* variable.
 - Data Type: \mathbb{R}
 - Structural Equation: *dist_headway_limit*
- *drag_scaled_air_mass_density*
 - Description: Calculates half of the *air_mass_density* variable via the *half_scale_factor_proxy* as the first step in calculating the drag force.
 - Data Type: \mathbb{R}
 - Structural Equation: *half_scale_factor_proxy* \times *air_mass_density*
- *lin_vel_dir*
 - Description: Normalisation of the *lin_vel_buff_A* variable.

- Data Type: \mathbb{R}^2
- Structural Equation: *lin_vel_buff_A* \times $\| \text{lin_vel_buff}_A \|^{-1}$
- *drag_force_dir*
 - Description: Negation of the *lin_vel_dir* variable.
 - Data Type: \mathbb{R}^2
 - Structural Equation: $- \text{lin_vel_dir}$
- *lin_vel_mag_squared*
 - Description: Dot product of the *lin_vel_buff_A* variable with itself.
 - Data Type: \mathbb{R}
 - Structural Equation: $\langle \text{lin_vel_buff}_A, \text{lin_vel_buff}_A \rangle$
- *dynamic_pressure*
 - Description: Calculates dynamic pressure from *drag_scaled_air_mass_density* and *lin_vel_mag_squared*.
 - Data Type: \mathbb{R}
 - Structural Equation: *drag_scaled_air_mass_density* \times *lin_vel_mag_squared*
- *drag_force_mag*
 - Description: Calculates drag force magnitude from *dynamic_pressure* and *drag_area_proxy_A*.
 - Data Type: \mathbb{R}
 - Structural Equation: *dynamic_pressure* \times *drag_area_proxy_A*
- *drag_force*
 - Description: Calculates drag force from the direction given by the *drag_force_mag* variable and the magnitude given by the *drag_force_mag* variable.
 - Data Type: \mathbb{R}^2
 - Structural Equation: *drag_force_dir* \times *drag_force_mag*
- *drag_torque_proxy*
 - Description: Proxy for the *drag_torque* variable.
 - Data Type: \mathbb{R}
 - Structural Equation: *drag_torque*
- *env_force*
 - Description: Sums the drag force with the collision forces contributed by *Point Mass Link* SCMs associated with this SCM.
 - Data Type: \mathbb{R}^2
 - Structural Equation: *drag_force* $+$ $\sum_{i=1}^{|\text{links}|} \text{actual_coll_force}_i$
- *env_torque*
 - Description: Sums the drag torque with the collision torques contributed by *Point Mass Link* SCMs associated with this SCM.
 - Data Type: \mathbb{R}
 - Structural Equation: *drag_torque_proxy* $+$ $\sum_{i=1}^{|\text{links}|} \text{actual_coll_torque}_i$
- *min_dist_headway*

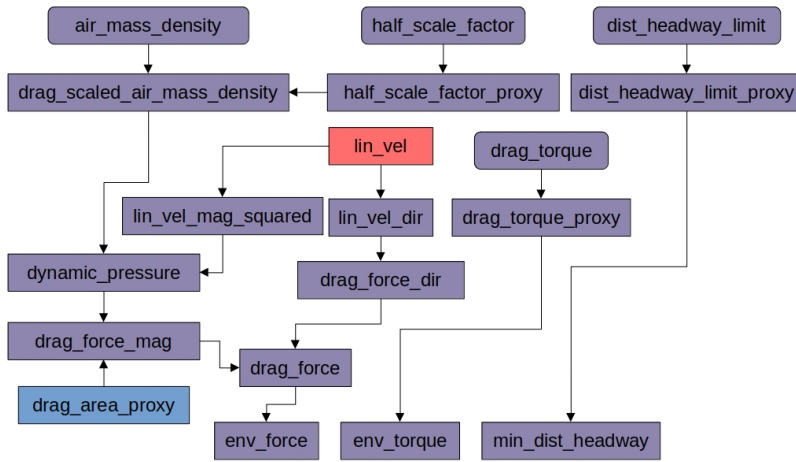


Figure 8: *Rectangular Rigid Body Entity SCM*

- Description: Finds the minimum of the distance headways contributed by *Point Mass Link* SCMs associated with this SCM, with a maximum distance headway given by the *dist_headway_limit_proxy* variable.
- Data Type: \mathbb{R}
- Structural Equation: $\min(\{drag_headway_limit_proxy\} \cup \bigcup_{i=1}^{|links|} dist_headway_i)$

A.6 Rectangular Rigid Body Link

Description Captures interactions between two rectangular rigid bodies in a shared environment. Most critically performs the collision computations for the two rigid bodies in question. Additionally computes distance headway between the two rigid bodies as this is frequently used within the driving domain as a safety metric (Nahata et al. 2021). Once again, variables belonging to the primary and secondary *Point Mass* SCMs associated with the link will be indicated via *A* and *B* subscripts respectively.

Graphical Layout Fig. 9 illustrates the graphical layout of the *Rectangular Rigid Link Body SCM*¹.

Variables

Hidden Exogenous:

- *no_coll_force*
 - Description: Represents collision force in the absence of a collision, i.e. none.
 - Data Type: \mathbb{R}^2
 - Distribution: *Degenerate*($[0, 0]^\top$)
- *no_coll_torque*
 - Description: Represents collision torque in the absence of a collision, i.e. none.
 - Data Type: \mathbb{R}
 - Distribution: *Degenerate*(0)

Endogenous:

- *mass_sum*
 - Description: The sum of the mass variables of both rectangular rigid bodies relevant to the link.
 - Data Type: \mathbb{R}
 - Structural Equation: $mass_A + mass_B$
- *mass_sum_recip*
 - Description: Reciprocal of the *mass_sum* variable.
 - Data Type: \mathbb{R}
 - Structural Equation: $mass_sum^{-1}$
- *coll*
 - Description: Determines whether *rect_A* and *rect_B* are in collision.
 - Data Type: \mathbb{B}
 - Structural Equation: Tests for collision between the 2D rectangular rigid bodies via separating axis theorem.
- *coll_contact*
 - Description: Determines the closest point of contact and direction of contact between *rect_A* and *rect_B*.
 - Data Type: $\mathbb{R}^2 \times \mathbb{R}^2$
 - Structural Equation: Projects each corner of each rectangular rigid body onto the other rectangular rigid body and takes the shortest projection in order to calculate the closest point and direction of contact between the rigid bodies.
- *coll_contact_pos*
 - Description: Extracts the point of contact from *coll_contact* variable.
 - Data Type: \mathbb{R}^2
 - Structural Equation: $coll_contact[0]$
- *coll_contact_dir*
 - Description: Extracts the direction of contact from *coll_contact* variable.

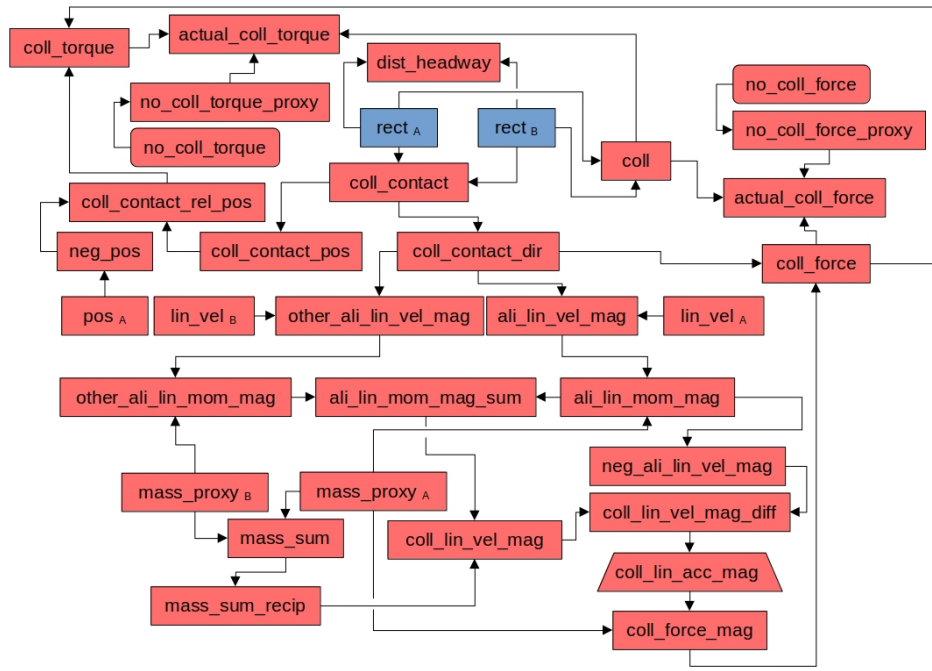


Figure 9: Rectangular Rigid Body Link SCM

- Data Type: \mathbb{R}^2
- Structural Equation: $coll_contact[1]$
- $ali_lin_vel_mag$
 - Description: Primary aligned linear velocity derived from the $coll_contact_dir$ and lin_vel_A variables.
 - Data Type: \mathbb{R}
 - Structural Equation: $\langle coll_contact_dir, lin_vel_A \rangle$
- $other_ali_lin_vel_mag$
 - Description: Secondary aligned linear velocity derived from the $coll_contact_dir$ and lin_vel_B variables.
 - Data Type: \mathbb{R}
 - Structural Equation: $\langle coll_contact_dir, lin_vel_B \rangle$
- $ali_lin_mom_mag$
 - Description: Primary aligned linear momentum derived from the $mass_A$ and $ali_lin_vel_mag$ variables.
 - Data Type: \mathbb{R}
 - Structural Equation: $mass_A \times ali_lin_vel_mag$
- $other_ali_lin_mom_mag$
 - Description: Secondary aligned linear momentum derived from the $mass_B$ and $other_ali_lin_vel_mag$ variables.
 - Data Type: \mathbb{R}
 - Structural Equation: $mass_B \times other_ali_lin_vel_mag$
- $ali_lin_mom_mag_sum$
 - Description: Combined aligned linear momentum derived from the $ali_lin_mom_mag$ and $other_ali_lin_mom_mag$ variables.
 - Data Type: \mathbb{R}
 - Structural Equation: $ali_lin_mom_mag + other_ali_lin_mom_mag$
- $coll_lin_vel_mag$
 - Description: Combined aligned linear velocity derived from the $mass_sum_recip$ and $ali_lin_mom_mag_sum$ variables.
 - Data Type: \mathbb{R}
 - Structural Equation: $mass_sum_recip \times ali_lin_mom_mag_sum$
- $neg_ali_lin_vel_mag$
 - Description: Negation of the $ali_lin_vel_mag$ variable.
 - Data Type: \mathbb{R}
 - Structural Equation: $-ali_lin_vel_mag$
- $coll_lin_vel_mag_diff$
 - Description: Difference between $coll_lin_vel_mag$ and $ali_lin_vel_mag$ derived by summing the $coll_lin_vel_mag$ and $neg_ali_lin_vel_mag$ variables.
 - Data Type: \mathbb{R}
 - Structural Equation: $coll_lin_vel_mag + neg_ali_lin_vel_mag$
- $coll_lin_acc_mag$
 - Description: Collision linear acceleration magnitude calculated from the $coll_lin_vel_mag_diff$ variable.
 - Data Type: \mathbb{R}
 - Structural Equation: $f_{V_{\pm\delta}}(coll_lin_vel_mag_diff)$
- $coll_force_mag$
 - Description: Collision force magnitude calculated from the $coll_lin_acc_mag$ variable.
 - Data Type: \mathbb{R}
 - Structural Equation: $coll_lin_acc_mag$

- Description: Collision force magnitude calculated from the $mass_A$ and $coll_lin_acc_mag$ variables.
- Data Type: \mathbb{R}
- Structural Equation: $mass_A \times coll_lin_acc_mag$
- $coll_force$
 - Description: Collision force constructed from the $coll_contact_dir$ and $coll_force_mag$ variables.
 - Data Type: \mathbb{R}^2
 - Structural Equation: $coll_contact_dir \times coll_force_mag$
- $no_coll_force_proxy$
 - Description: Proxy for the no_coll_force variable.
 - Data Type: \mathbb{R}^2
 - Structural Equation: no_coll_force
- $actual_coll_force$
 - Description: Selects between the $coll_force$ and $no_coll_force_proxy$ variables depending upon the $coll$ variable.
 - Data Type: \mathbb{R}^2
 - Structural Equation: $\begin{cases} coll_force & coll \\ no_coll_force_proxy & \neg coll \end{cases}$
- neg_pos
 - Description: Negation of the pos_A variable.
 - Data Type: \mathbb{R}^2
 - Structural Equation: $\neg pos_A$
- $coll_contact_rel_pos$
 - Description: Collision contact point relative to the primary rectangular rigid body, derived from the $coll_contact_pos$ and neg_pos variables.
 - Data Type: \mathbb{R}^2
 - Structural Equation: $coll_contact_pos + neg_pos$
- $coll_torque$
 - Description: Collision torque derived from the $coll_force$ and $coll_contact_rel_pos$ variables.
 - Data Type: \mathbb{R}
 - Structural Equation: $\begin{matrix} & coll_force[1] & \times \\ coll_contact_rel_pos[0] & + & coll_force[0] & \times \\ & coll_contact_rel_pos[1] & \times \end{matrix}$
- $no_coll_torque_proxy$
 - Description: Proxy for the no_coll_torque variable.
 - Data Type: \mathbb{R}
 - Structural Equation: no_coll_torque
- $actual_coll_torque$
 - Description: Selects between the $coll_torque$ and $no_coll_torque_proxy$ variables depending upon the $coll$ variable.
 - Data Type: \mathbb{R}
 - Structural Equation: $\begin{cases} coll_torque & coll \\ no_coll_torque_proxy & \neg coll \end{cases}$
- $dist_headway$

- Description: Calculates the distance headway for $rect_A$ with $rect_B$ as an obstacle, up to a predefined limit (e.g. 100 m).
- Data Type: \mathbb{R}
- Structural Equation: Determines whether the secondary rectangular rigid body lies in the path of the primary rectangular rigid body by comparing the relative position of the secondary rigid body against the heading of the primary rigid body. Provided the secondary rigid body is in the path of the primary rigid body, it's distance is calculated by projecting the aforementioned relative position onto the vector indicating the heading of the primary rigid body. Should the resulting value be below zero, above the predefined limit, or if the secondary rigid body lies outside of the primary rigid body's path, the predefined limit will be returned, otherwise the projected length will be.

A.7 Pedestrian

Description Inherits from the *Point Mass* SCM to represent a pedestrian agent, be it a human or robot. Functionally speaking just a wrapper *Point Mass* SCM, as unlike the *FWD Car* SCM of the autonomous driving architecture, additional functionality was not required above the base *Point Mass* SCM at the time of the architecture's development.

Graphical Layout N/A

Variables N/A

A.8 FWD Car

Description Inherits from the *Rectantular Rigid Body* SCM to represent a road vehicle, in particular one that has front wheel drive (FWD). This SCM provides forces and torques as output to the underlying *Rectantular Rigid Body* SCM, instead providing variables for motor torque and steering as input. In order to calculate the forces and torques required, the SCM utilises these two inputs and treats the represented object as a dynamic bicycle (Guiggiani 2018), a simple means by which one can model a variety of vehicles.

Graphical Layout Fig. 10 illustrates the graphical layout of the *FWD Car* SCM.

Variables

Hidden Exogenous:

- $wheel_radius$
 - Description: Radius of the vehicle's wheels.
 - Data Type: \mathbb{R}
 - Distribution: $\langle \text{initialisation parameter} \rangle$
- $axle_dist$
 - Description: Distance of the wheel axes from the centre of the vehicle.
 - Data Type: \mathbb{R}
 - Distribution: $\langle \text{initialisation parameter} \rangle$
- $cornering_stiffness$
 - Description: Cornering stiffness of the tires.

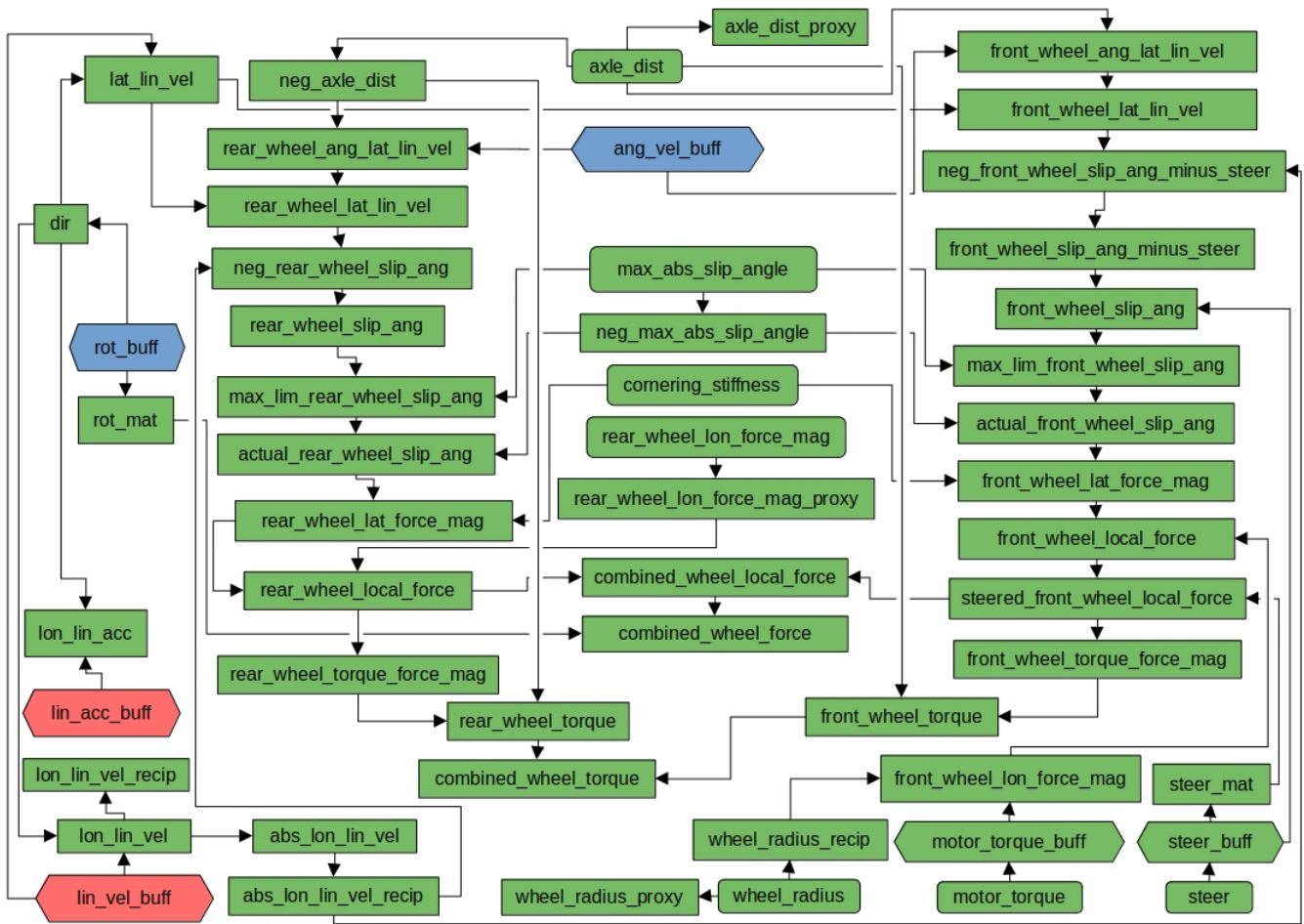


Figure 10: FWD Car SCM

- Data Type: \mathbb{R}
 - Distribution: $\langle \text{initialisation parameter} \rangle$
 - *max_abs_slip_angle*
 - Description: Maximum slip angle. In reality after a certain point cornering forces turn into friction forces, but this is a simplification of the physics.
 - Data Type: \mathbb{R}
 - Distribution: $\langle \text{initialisation parameter} \rangle$
 - *rear_wheel_lon_force_mag*
 - Description: Longitudinal force from the rear wheels. Fixed at zero because it is assumed the rear wheels freely spin without resistance.
 - Data Type: \mathbb{R}
 - Distribution: *Degenerate*(0)
- Socket:
- *motor_torque*
 - Description: Front wheel axle motor torque actuating the vehicle.
 - Data Type: \mathbb{R}
 - *steer*
 - Description: Front wheel steering actuating the vehicle.
 - Data Type: \mathbb{R}
 - Default Distribution: *Degenerate*(0)
 - Default Distribution: *Degenerate*(0)
- Endogenous:
- *wheel_radius_proxy*
 - Description: Proxy for the *wheel_radius* variable.
 - Data Type: \mathbb{R}
 - Structural Equation: *wheel_radius*
 - *wheel_radius_recip*
 - Description: Reciprocal of the *wheel_radius* variable.
 - Data Type: \mathbb{R}
 - Structural Equation: *wheel_radius*⁻¹
 - *axle_dist_proxy*
 - Description: Proxy for the *axle_dist* variable.
 - Data Type: \mathbb{R}

- Structural Equation: $axle_dist$
- neg_axle_dist
 - Description: Negation of the $axle_dist$ variable.
 - Data Type: \mathbb{R}
 - Structural Equation: $-axle_dist$
- $neg_max_abs_slip_angle$
 - Description: Negation of the $max_abs_slip_angle$ variable.
 - Data Type: \mathbb{R}
 - Structural Equation: $-max_abs_slip_angle$
- dir
 - Description: Directional vector derived from the rot_buff variable.
 - Data Type: \mathbb{R}^2
 - Structural Equation: $[\cos(rot_buff), \sin(rot_buff)]^\top$
- lon_lin_acc
 - Description: Longitudinal linear acceleration derived by projecting the lin_acc_buff variable onto the dir variable.
 - Data Type: \mathbb{R}
 - Structural Equation: $\langle lin_acc_buff, dir \rangle$
- lon_lin_vel
 - Description: Longitudinal linear velocity derived by projecting the lin_vel_buff variable onto the dir variable.
 - Data Type: \mathbb{R}
 - Structural Equation: $\langle lin_vel_buff, dir \rangle$
- $lon_lin_vel_recip$
 - Description: Reciprocal of the lon_lin_vel variable.
 - Data Type: \mathbb{R}
 - Structural Equation: $lon_lin_vel^{-1}$
- $abs_lon_lin_vel$
 - Description: Absolute of the lon_lin_vel variable.
 - Data Type: \mathbb{R}
 - Structural Equation: $|lon_lin_vel|$
- $abs_lon_lin_vel_recip$
 - Description: Reciprocal of the $abs_lon_lin_vel$ variable.
 - Data Type: \mathbb{R}
 - Structural Equation: $abs_lon_lin_vel^{-1}$
- lat_lin_vel
 - Description: Lateral linear velocity derived via the exterior product of the lin_vel_buff and dir variables and the sine rule.
 - Data Type: \mathbb{R}
 - Structural Equation: $lin_vel_buff[1] \times dir[0] + lin_vel_buff[0] \times dir[1]$
- $motor_torque_buff$
 - Description: Buffer for the $motor_torque$ variable.
- Data Type: \mathbb{R}
- Structural Equation: $f_{V_B}(motor_torque)$
- $front_wheel_lon_force_mag$
 - Description: Longitudinal force from the front wheels calculated from the $wheel_radius_recip$ and $motor_torque_buff$ variables.
 - Data Type: \mathbb{R}
 - Structural Equation: $wheel_radius_recip \times motor_torque_buff$
- $rear_wheel_lon_force_mag_proxy$
 - Description: Proxy for the $rear_wheel_lon_force_mag$ variable.
 - Data Type: \mathbb{R}
 - Structural Equation: $rear_wheel_lon_force_mag$
- $front_wheel_ang_lat_lin_vel$
 - Description: Calculates the lateral linear velocity at the front wheel axle from angular velocity via the ang_vel_buff and $axle_dist$ variables.
 - Data Type: \mathbb{R}
 - Structural Equation: $ang_vel_buff \times axle_dist$
- $front_wheel_lat_lin_vel$
 - Description: Calculates the total lateral linear velocity at the front wheel axle via the lat_lin_vel and $front_wheel_ang_lat_lin_vel$ variables.
 - Data Type: \mathbb{R}
 - Structural Equation: $lat_lin_vel + front_wheel_ang_lat_lin_vel$
- $neg_front_wheel_slip_ang_minus_steer$
 - Description: Calculates the negative wheel slip at the front wheels, not accounting for steering, via the $front_wheel_lat_lin_vel$ and $abs_lon_lin_vel_recip$ variables.
 - Data Type: \mathbb{R}
 - Structural Equation: $front_wheel_lat_lin_vel \times abs_lon_lin_vel_recip$
- $front_wheel_slip_ang_minus_steer$
 - Description: Calculates the wheel slip at the front wheels, not accounting for steering, via the $neg_front_wheel_slip_ang_minus_steer$ variable.
 - Data Type: \mathbb{R}
 - Struc. Eq.: $-neg_front_wheel_slip_ang_minus_steer$
- $steer_buff$
 - Description: Buffer for the $steer$ variable.
 - Data Type: \mathbb{R}
 - Structural Equation: $f_{V_B}(steer)$
- $front_wheel_slip_ang$
 - Description: Calculates the wheel slip at the front wheels, via the $front_wheel_slip_ang_minus_steer$ and $steer_buff$ variables.
 - Data Type: \mathbb{R}

- Structural Equation: $front_wheel_slip_ang_minus_steer + steer_buff$
- $max_lim_front_wheel_slip_ang$
 - Description: Maximum limited wheel slip at the front wheels, via the $front_wheel_slip_ang$ and $max_abs_slip_angle$ variables.
 - Data Type: \mathbb{R}
 - Structural Equation: $\min\{front_wheel_slip_ang, max_abs_slip_angle\}$
- $actual_front_wheel_slip_ang$
 - Description: Maximum & minimum limited wheel slip at the front wheels, via the $max_lim_front_wheel_slip_ang$ and $neg_max_abs_slip_angle$ variables.
 - Data Type: \mathbb{R}
 - Structural Equation: $\max\{max_lim_front_wheel_slip_ang, neg_max_abs_slip_angle\}$
- $front_wheel_lat_force_mag$
 - Description: Lateral force from the front wheels calculated from the $actual_front_wheel_slip_ang$ and $cornering_stiffness$ variables.
 - Data Type: \mathbb{R}
 - Structural Equation: $actual_front_wheel_slip_ang \times cornering_stiffness$
- $rear_wheel_ang_lat_lin_vel$
 - Description: Calculates the lateral linear velocity at the rear wheel axle from angular velocity via the ang_vel_buff and neg_axle_dist variables.
 - Data Type: \mathbb{R}
 - Structural Equation: $ang_vel_buff \times neg_axle_dist$
- $rear_wheel_lat_lin_vel$
 - Description: Calculates the total lateral linear velocity at the rear wheel axle via the lat_lin_vel and $rear_wheel_ang_lat_lin_vel$ variables.
 - Data Type: \mathbb{R}
 - Structural Equation: $lat_lin_vel + rear_wheel_ang_lat_lin_vel$
- $neg_rear_wheel_slip_ang$
 - Description: Calculates the negative wheel slip at the front wheels, via the $rear_wheel_lat_lin_vel$ and $abs_lon_lin_vel_recip$ variables.
 - Data Type: \mathbb{R}
 - Structural Equation: $rear_wheel_lat_lin_vel \times abs_lon_lin_vel_recip$
- $rear_wheel_slip_ang$
 - Description: Calculates the wheel slip at the rear wheels, via the $neg_rear_wheel_slip_ang$ variable.
 - Data Type: \mathbb{R}
 - Structural Equation: $-neg_rear_wheel_slip_ang$
- $max_lim_rear_wheel_slip_ang$
 - Description: Maximum limited wheel slip at the rear wheels, via the $rear_wheel_slip_ang$ and $max_abs_slip_angle$ variables.
 - Data Type: \mathbb{R}
 - Structural Equation: $\min\{rear_wheel_slip_ang, max_abs_slip_angle\}$
- $actual_rear_wheel_slip_ang$
 - Description: Maximum & minimum limited wheel slip at the rear wheels, via the $max_lim_rear_wheel_slip_ang$ and $neg_max_abs_slip_angle$ variables.
 - Data Type: \mathbb{R}
 - Structural Equation: $\max\{max_lim_rear_wheel_slip_ang, neg_max_abs_slip_angle\}$
- $rear_wheel_lat_force_mag$
 - Description: Lateral force from the rear wheels calculated from the $actual_rear_wheel_slip_ang$ and $cornering_stiffness$ variables.
 - Data Type: \mathbb{R}
 - Structural Equation: $actual_rear_wheel_slip_ang \times cornering_stiffness$
- $front_wheel_local_force$
 - Description: Constructs the force vector at the front wheel axle in the local frame from the $front_wheel_lon_force_mag$ and $front_wheel_lat_force_mag$ variables.
 - Data Type: \mathbb{R}^2
 - Structural Equation: $[front_wheel_lon_force_mag, front_wheel_lat_force_mag]^T$
- $steer_mat$
 - Description: Constructs a rotation matrix from the $steer_buff$ variable.
 - Data Type: $\mathbb{R}^{2 \times 2}$
 - Structural Equation: $\begin{bmatrix} \cos(steer_buff) & -\sin(steer_buff) \\ \sin(steer_buff) & \cos(steer_buff) \end{bmatrix}$
- $steered_front_wheel_local_force$
 - Description: Force vector at the front wheel axle in the local frame given by the $front_wheel_local_force$ variable rotated by the $steer_buff$ variable via the $steer_mat$ variable.
 - Data Type: \mathbb{R}^2
 - Structural Equation: $steer_mat \times front_wheel_local_force$
- $rear_wheel_local_force$
 - Description: Constructs the force vector at the rear wheel axle in the local frame from the $rear_wheel_lon_force_mag$ and $rear_wheel_lat_force_mag$ variables.
 - Data Type: \mathbb{R}^2
 - Structural Equation: $[rear_wheel_lon_force_mag, rear_wheel_lat_force_mag]^T$
- $front_wheel_torque_force_mag$

- Description: The lateral component of the *steered_front_wheel_local_force* variable that affects the vehicle’s overall torque.
- Data Type: \mathbb{R}
- Structural Equation: *steered_front_wheel_local_force*[1]
- *front_wheel_torque*
 - Description: The torque provided by the *front_wheel_torque_force_mag* variable multiplied by the *axle_dist* variable.
 - Data Type: \mathbb{R}
 - Structural Equation: *front_wheel_torque_force_mag* \times *axle_dist*
- *rear_wheel_torque_force_mag*
 - Description: The lateral component of the *rear_wheel_local_force* variable that affects the vehicle’s overall torque.
 - Data Type: \mathbb{R}
 - Structural Equation: *rear_wheel_local_force*[1]
- *rear_wheel_torque*
 - Description: The torque provided by the *rear_wheel_torque_force_mag* variable multiplied by the *neg_axle_dist* variable.
 - Data Type: \mathbb{R}
 - Structural Equation: *rear_wheel_torque_force_mag* \times *neg_axle_dist*
- *combined_wheel_local_force*
 - Description: Combines the local wheel forces provided by the *steered_front_wheel_local_force* and *rear_wheel_local_force* variables.
 - Data Type: \mathbb{R}^2
 - Structural Equation: *steered_front_wheel_local_force* + *rear_wheel_local_force*
- *rot_mat*
 - Description: Constructs a rotation matrix from the *rot_buff* variable.
 - Data Type: $\mathbb{R}^{2 \times 2}$
 - Structural Equation:
$$\begin{bmatrix} \cos(\text{rot_buff}) & -\sin(\text{rot_buff}) \\ \sin(\text{rot_buff}) & \cos(\text{rot_buff}) \end{bmatrix}$$
- *combined_wheel_force*
 - Description: Rotates the *combined_wheel_local_force* variable into the global frame via the *rot_mat* variable.
 - Data Type: \mathbb{R}^2
 - Structural Equation: *rot_mat* + *combined_wheel_local_force*
- *combined_wheel_torque*
 - Description: Combines the local wheel torques provided by the *front_wheel_torque* and *rear_wheel_torque* variables.
 - Data Type: \mathbb{R}
 - Structural Equation: *front_wheel_torque* + *rear_wheel_torque*

A.9 Goal Force Control Pedestrian

Description Provides a control mechanism which outputs a force in return for giving a goal node id and a goal time as input. The node id corresponds to a vertex within a 2D spatial graph. The controller simply calculates a force magnitude proportional to the distance the node is from the position given by the *Pedestrian* SCM, and inversely proportional to the difference between the current time and the goal time. This magnitude is limited in order to ensure the resulting force is not unrealistic for what a human / robot might be capable of. Meanwhile the force direction is calculated as the unit vector pointing from the current position to the goal node position. The combination of the force magnitude and direction provides the output for the SCM which can then be fed into the *Pedestrian* SCM.

Graphical Layout Fig. 11 illustrates the graphical layout of the *Goal Force Control Pedestrian* SCM.

Variables

Hidden Exogenous:

- *min_act_horizon_secs*
 - Description: Minimum actuation horizon in seconds.
 - Data Type: \mathbb{R}
 - Distribution: *Degenerate*(1)
- *max_goal_force_mag*
 - Description: Maximum goal force magnitude.
 - Data Type: \mathbb{R}
 - Distribution: \langle initialisation parameter \rangle

Socket:

- *action*
 - Description: Pedestrian action.
 - Data Type: $\mathbb{Z} \times \mathcal{T}$
 - Default Distribution: *Degenerate*([0, 0]^T)
- *ped_force*
 - Description: Output force from controller for pedestrian. Will be connected to *actual_goal_force* upon controller initialisation.
 - Data Type: \mathbb{R}^2
 - Default Distribution: *Degenerate*([0, 0]^T)
- *pos*
 - Description: Pedestrian position.
 - Data Type: \mathbb{R}^2
 - Default Distribution: *Degenerate*([0, 0]^T)
- *lin_vel*
 - Description: Pedestrian linear velocity.
 - Data Type: \mathbb{R}^2
 - Default Distribution: *Degenerate*([0, 0]^T)
- *mass*
 - Description: Pedestrian mass.
 - Data Type: \mathbb{R}
 - Default Distribution: *Degenerate*(0)

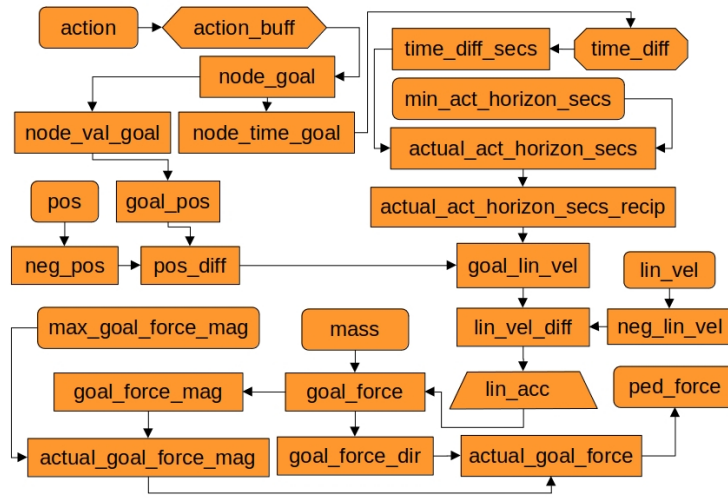


Figure 11: Goal Force Control Pedestrian SCM

Endogenous:

- *action_buff*
 - Description: Buffer for the *action* variable.
 - Data Type: $\mathbb{Z} \times \mathcal{T}$
 - Structural Equation: $f_{V_B}(action)$
- *node_val_goal*
 - Description: Gets the value part of the *node_goal* variable.
 - Data Type: \mathbb{Z}
 - Structural Equation: $node_goal[0]$
- *node_time_goal*
 - Description: Gets the time part of the *node_goal* variable.
 - Data Type: \mathcal{T}
 - Structural Equation: $node_goal[1]$
- *goal_pos*
 - Description: Goal position derived from the graphical roadmap and the *node_val_goal* variable.
 - Data Type: \mathbb{R}^2
 - Structural Equation: Retrieves the node associated with the provided id in the graphical roadmap and returns its position.
- *neg_pos*
 - Description: Negation of the *pos* variable.
 - Data Type: \mathbb{R}^2
 - Structural Equation: $-pos$
- *pos_diff*
 - Description: Position difference calculated from the *goal_pos* and *neg_pos* variables.
 - Data Type: \mathbb{R}^2
 - Structural Equation: $goal_pos + neg_pos$
- *time_diff*
 - Description: Time difference calculated from the *node_time_goal* variable. Note \mathcal{D} is a duration data type.
 - Data Type: \mathcal{D}
 - Structural Equation: $f_{V_{\Delta T}}(node_time_goal)$
- *time_diff_secs*
 - Description: Time difference in seconds calculated from the *time_diff* variable.
 - Data Type: \mathbb{R}
 - Structural Equation: Converts from the duration data type to seconds captured as a real number.
- *actual_act_horizon_secs*
 - Description: Actual actuation horizon in seconds, derived from the maximum of the *time_diff_secs* and *min_act_horizon_secs* variables.
 - Data Type: \mathbb{R}
 - Structural Equation: $\max\{time_diff_secs, min_act_horizon_secs\}$
- *actual_act_horizon_secs_recip*
 - Description: Reciprocal of the *actual_act_horizon_secs* variable.
 - Data Type: \mathbb{R}
 - Structural Equation: $actual_act_horizon_secs^{-1}$

- *goal_lin_vel*
 - Description: Goal linear velocity calculated from *pos_diff* and *actual_act_horizon_secs_recip* variables.
 - Data Type: \mathbb{R}^2
 - Structural Equation:
$$\frac{pos_diff}{actual_act_horizon_secs_recip} \times$$
- *neg_lin_vel*
 - Description: Negation of the *lin_vel* variable.
 - Data Type: \mathbb{R}^2
 - Structural Equation: $-lin_vel$
- *lin_vel_diff*
 - Description: Linear velocity difference calculated from the *goal_lin_vel* and *neg_lin_vel* variables.
 - Data Type: \mathbb{R}^2
 - Structural Equation: $goal_lin_vel + neg_lin_vel$
- *lin_acc*
 - Description: Linear acceleration calculated from *lin_vel_diff*.
 - Data Type: \mathbb{R}^2
 - Structural Equation: $f_{V \rightarrow \delta}(lin_vel_diff)$
- *goal_force*
 - Description: Goal force calculated from *lin_acc* and *mass*.
 - Data Type: \mathbb{R}^2
 - Structural Equation: $lin_acc \times mass$
- *goal_force_mag*
 - Description: Calculates the norm of the *goal_force* variable.
 - Data Type: \mathbb{R}
 - Structural Equation: $\|goal_force\|$
- *actual_goal_force_mag*
 - Description: Maximum limited goal force magnitude, via the *goal_force_mag* and *max_goal_force_mag* variables.
 - Data Type: \mathbb{R}
 - Structural Equation: $\min\{goal_force_mag, max_goal_force_mag\}$
- *goal_force_dir*
 - Description: Normalisation of the *goal_force* variable.
 - Data Type: \mathbb{R}^2
 - Structural Equation: $goal_force \times \|goal_force\|^{-1}$
- *actual_goal_force*
 - Description: Maximum limited goal force derived from the *goal_force_dir* and *actual_goal_force_mag* variables.
 - Data Type: \mathbb{R}^2
 - Structural Equation:
$$goal_force_dir \times actual_goal_force_mag$$

A.10 Motor Torque Control FWD Car

Description Provides a control mechanism which outputs motor torque in return for giving a goal speed and a goal time as input. From the difference between the longitudinal linear velocity given by the *FWD Car SCM* and the goal velocity, and the difference between the current time and the goal time it is possible to calculate the necessary acceleration. Using the mass of the *FWD Car SCM* one can calculate the required force, before making adjustments to the force to account for environment forces also acting upon the *FWD Car SCM*. From the calculated force and the wheel radius of the vehicle one can at last approximate the output motor torque which can then be fed into the *FWD Car SCM*.

Graphical Layout Fig. 12 illustrates the graphical layout of the *Motor Torque Control FWD Car SCM*.

Variables

Hidden Exogenous:

- *max_motor_torque*
 - Description: Maximum motor torque.
 - Data Type: \mathbb{R}
 - Distribution: $\langle \text{initialisation parameter} \rangle$
- *min_motor_torque*
 - Description: Minimum motor torque.
 - Data Type: \mathbb{R}
 - Distribution: $\langle \text{initialisation parameter} \rangle$
- *min_act_horizon_secs*
 - Description: Maximum actuation horizon in seconds.
 - Data Type: \mathbb{R}
 - Distribution: $Degenerate(1)$

Socket:

- *action*
 - Description: Vehicle action.
 - Data Type: $(\mathbb{R} \times \mathcal{T}) \times (\mathbb{Z} \times \mathcal{T})$
 - Default Distribution: $Degenerate(\llbracket [0, 0]^\top, [0, 0]^\top \rrbracket)$
- *motor_torque*
 - Description: Output motor torque from controller for vehicle. Will be connected to *actual_motor_torque* upon controller initialisation.
 - Data Type: \mathbb{R}
 - Default Distribution: $Degenerate(0)$
- *speed*
 - Description: Vehicle speed.
 - Data Type: \mathbb{R}
 - Default Distribution: $Degenerate(0)$
- *mass*
 - Description: Vehicle mass.
 - Data Type: \mathbb{R}
 - Default Distribution: $Degenerate(0)$
- *wheel_radius*

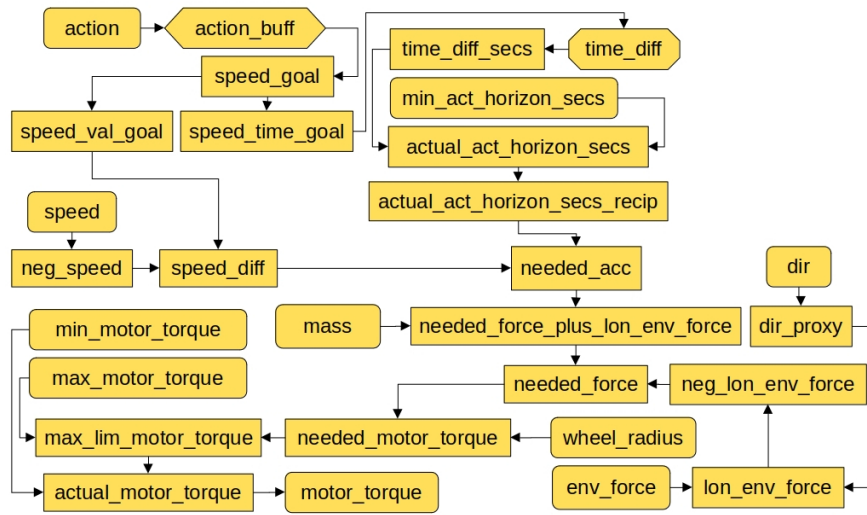


Figure 12: Motor Torque Control FWD Car SCM

- Description: Vehicle wheel radius.
 - Data Type: \mathbb{R}
 - Default Distribution: $Degenerate(0)$
 - *dir*
 - Description: Vehicle direction.
 - Data Type: \mathbb{R}^2
 - Default Distribution: $Degenerate([0, 0]^\top)$
 - *env_force*
 - Description: Total environment forces affecting vehicle.
 - Data Type: \mathbb{R}^2
 - Default Distribution: $Degenerate([0, 0]^\top)$
- Endogenous:
- *action_buff*
 - Description: Buffer for the *action* variable.
 - Data Type: $(\mathbb{R} \times \mathcal{T}) \times (\mathbb{Z} \times \mathcal{T})$
 - Structural Equation: $f_{V_B}(action)$
 - *speed_goal*
 - Description: Gets the speed goal part of the *action_buff* variable.
 - Data Type: $\mathbb{R} \times \mathcal{T}$
 - Structural Equation: $action_buff[0]$
 - *speed_val_goal*
 - Description: Gets the value part of the *speed_goal* variable.
 - Data Type: \mathbb{R}
 - Structural Equation: $speed_goal[0]$
 - *speed_time_goal*
 - Description: Gets the time part of the *speed_goal* variable.
 - Data Type: \mathcal{T}
 - *time_diff*
 - Description: Time difference calculated from the *node_time_goal* variable. Note \mathcal{D} is a duration data type.
 - Data Type: \mathcal{D}
 - Structural Equation: $f_{V_{\Delta T}}(node_time_goal)$
 - *time_diff_secs*
 - Description: Time difference in seconds calculated from the *time_diff* variable.
 - Data Type: \mathbb{R}
 - Structural Equation: Converts from the duration data type to seconds captured as a real number.
 - *actual_act_horizon_secs*
 - Description: Actual actuation horizon in seconds, derived from the maximum of the *time_diff_secs* and *min_act_horizon_secs* variables.
 - Data Type: \mathbb{R}
 - Structural Equation: $\max\{time_diff_secs, min_act_horizon_secs\}$
 - *actual_act_horizon_secs_recip*
 - Description: Reciprocal of the *actual_act_horizon_secs* variable.
 - Data Type: \mathbb{R}
 - Structural Equation: $actual_act_horizon_secs^{-1}$
 - *neg_speed*
 - Description: Negation of the *speed* variable.
 - Data Type: \mathbb{R}
 - Structural Equation: $-speed$
 - *speed_diff*
 - Description: Speed difference calculated from the *goal_speed* and *neg_speed* variables.
 - *needed_force_plus_lon_env_force*
 - Structural Equation: $speed_goal[1]$
 - *needed_force*
 - Structural Equation: $needed_force_plus_lon_env_force - neg_lon_env_force$
 - *needed_motor_torque*
 - Structural Equation: $needed_force / wheel_radius$
 - *motor_torque*
 - Structural Equation: $needed_motor_torque$
 - *actual_motor_torque*
 - Structural Equation: $min(max(needed_motor_torque, min_motor_torque), max_motor_torque, max_lim_motor_torque)$
 - *lon_env_force*
 - Structural Equation: $needed_force_plus_lon_env_force + neg_lon_env_force$
 - *neg_lon_env_force*
 - Structural Equation: dir_proxy

- Data Type: \mathbb{R}
- Structural Equation: $goal_speed + neg_speed$
- *dir_proxy*
 - Description: Proxy for the *dir* variable.
 - Data Type: \mathbb{R}^2
 - Structural Equation: *dir*
- *needed_acc*
 - Description: Needed acceleration based upon the *speed_diff* and *actual_act_horizon_secs_recip* variables.
 - Data Type: \mathbb{R}
 - Structural Equation: $speed_diff \times actual_act_horizon_secs_recip$
- *needed_force_plus_lon_env_force*
 - Description: Needed force, not accounting for environment forces, based upon the *needed_acc* and *mass* variables.
 - Data Type: \mathbb{R}
 - Structural Equation: $needed_acc \times mass$
- *lon_env_force*
 - Description: Longitudinal environment forces derived by projecting the *env_force* variable onto the *dir_proxy* variable.
 - Data Type: \mathbb{R}
 - Structural Equation: $\langle dir_proxy, env_force \rangle$
- *neg_lon_env_force*
 - Description: Negation of the *lon_env_force* variable.
 - Data Type: \mathbb{R}
 - Structural Equation: $-lon_env_force$
- *needed_force*
 - Description: Needed force based upon the *needed_force_plus_lon_env_force* and *neg_lon_env_force* variables.
 - Data Type: \mathbb{R}
 - Structural Equation: $needed_force_plus_lon_env_force + neg_lon_env_force$
- *needed_motor_torque*
 - Description: Needed motor torque based upon the *needed_force* and *wheel_radius* variables.
 - Data Type: \mathbb{R}
 - Structural Equation: $needed_force \times wheel_radius$
- *max_lim_motor_torque*
 - Description: Maximum limited motor torque, via the *needed_motor_torque* and *max_motor_torque* variables.
 - Data Type: \mathbb{R}
 - Structural Equation: $\min\{needed_motor_torque, max_motor_torque\}$
- *actual_motor_torque*

- Description: Maximum & minimum limited motor torque, via the *max_lim_motor_torque* and *min_motor_torque* variables.
- Data Type: \mathbb{R}
- Structural Equation: $\max\{max_lim_motor_torque, min_motor_torque\}$

A.11 Steer Control FWD Car

Description Provides a control mechanism which outputs steer in return for giving a goal lane id and a goal time as input. In order to calculate the steering first the expected position of the rectangular rigid body is calculated for a predefined future horizon. This is then projected onto the closest point of the central path of the lane associated with the goal lane id. The expected position combined with the projected position and current position given by the *FWD Car* SCM provide an angle error. This angle error, along with its derivative are then used as inputs to a proportional-derivative controller (Lipták 2013), with the steering as the output which is then fed into the *FWD Car* SCM.

Graphical Layout Fig. 13 illustrates the graphical layout of the *Steer Control FWD Car* SCM.

Variables

Hidden Exogenous:

- *max_steer*
 - Description: Maximum steer.
 - Data Type: \mathbb{R}
 - Distribution: $\langle \text{initialisation parameter} \rangle$
- *min_act_horizon_secs*
 - Description: Maximum actuation horizon in seconds.
 - Data Type: \mathbb{R}
 - Distribution: *Degenerate*(1)
- *k_p*
 - Description: Proportional gain.
 - Data Type: \mathbb{R}
 - Distribution: *Degenerate*(0.2)
- *k_d*
 - Description: Derivative gain.
 - Data Type: \mathbb{R}
 - Distribution: *Degenerate*(0)

Socket:

- *action*
 - Description: Vehicle action.
 - Data Type: $(\mathbb{R} \times \mathcal{T}) \times (\mathbb{Z} \times \mathcal{T})$
 - Default Distribution: *Degenerate*($[[[0, 0]^\top, [0, 0]^\top]$)
- *steer*
 - Description: Output steer from controller for vehicle. Will be connected to *actual_steer* upon controller initialisation.
 - Data Type: \mathbb{R}

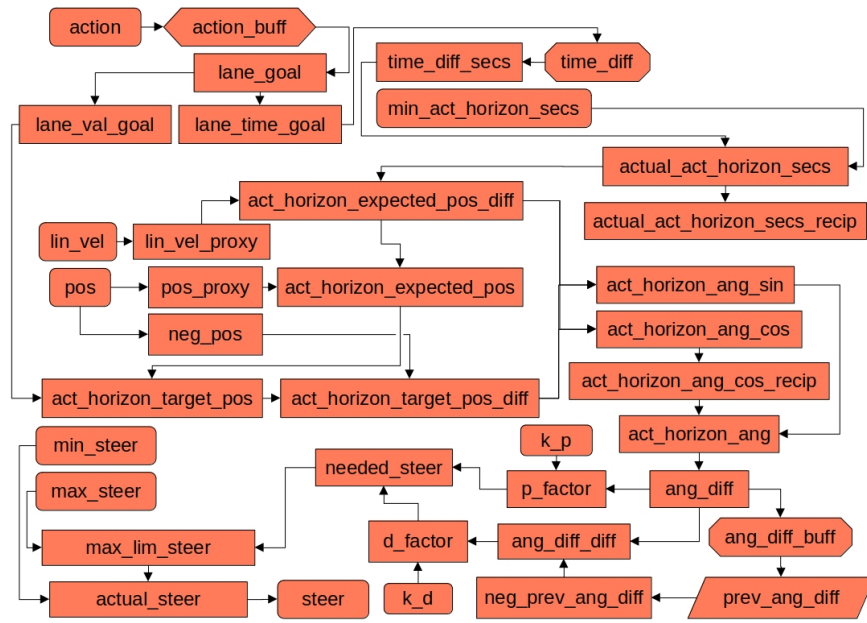


Figure 13: Steer Control FWD Car SCM

- Default Distribution: $Degenerate(0)$
- *pos*
 - Description: Vehicle position.
 - Data Type: \mathbb{R}^2
 - Default Distribution: $Degenerate([0, 0]^T)$
- *lin_vel*
 - Description: Vehicle linear velocity.
 - Data Type: \mathbb{R}^2
 - Default Distribution: $Degenerate([0, 0]^T)$
- Endogenous:
 - *action_buff*
 - Description: Buffer for the *action* variable.
 - Data Type: $(\mathbb{R} \times \mathcal{T}) \times (\mathbb{Z} \times \mathcal{T})$
 - Structural Equation: $f_{V_B}(action)$
 - *lane_goal*
 - Description: Gets the lane goal part of the *action_buff* variable.
 - Data Type: $\mathbb{Z} \times \mathcal{T}$
 - Structural Equation: $action_buff[1]$
 - *lane_val_goal*
 - Description: Gets the value part of the *lane_goal* variable.
 - Data Type: \mathbb{Z}
 - Structural Equation: $lane_goal[0]$
 - *lane_time_goal*
 - Description: Gets the time part of the *lane_goal* variable.
 - Data Type: \mathcal{T}
 - Structural Equation: $lane_goal[1]$
 - *min_steer*
 - Description: Minimum steer, calculated as the negation of the *max_steer* variable.
 - Data Type: \mathbb{R}
 - Distribution: $-max_steer$
 - *time_diff*
 - Description: Time difference calculated from the *node_time_goal* variable. Note \mathcal{D} is a duration data type.
 - Data Type: \mathcal{D}
 - Structural Equation: $f_{V_{\Delta T}}(node_time_goal)$
 - *time_diff_secs*
 - Description: Time difference in seconds calculated from the *time_diff* variable.
 - Data Type: \mathbb{R}
 - Structural Equation: Converts from the duration data type to seconds captured as a real number.
 - *actual_act_horizon_secs*
 - Description: Actual actuation horizon in seconds, derived from the maximum of the *time_diff_secs* and *min_act_horizon_secs* variables.
 - Data Type: \mathbb{R}
 - Structural Equation: $\max\{time_diff_secs, min_act_horizon_secs\}$
 - *actual_act_horizon_secs_recip*
 - Description: Reciprocal of the *actual_act_horizon_secs* variable.

- Data Type: \mathbb{R}
- Structural Equation: $actual_act_horizon_secs^{-1}$
- *pos_proxy*
 - Description: Proxy for the *pos* variable.
 - Data Type: \mathbb{R}^2
 - Structural Equation: *pos*
- *lin_vel_proxy*
 - Description: Proxy for the *lin_vel* variable.
 - Data Type: \mathbb{R}^2
 - Structural Equation: *lin_vel*
- *act_horizon_expected_pos_diff*
 - Description: Expected position difference by the end of the actuation horizon, calculated as the product of the *lin_vel_proxy* and *actual_act_horizon_secs* variables.
 - Data Type: \mathbb{R}^2
 - Structural Equation: $lin_vel_proxy \times actual_act_horizon_secs$
- *act_horizon_expected_pos*
 - Description: Expected position by the end of the actuation horizon, calculated as the sum of the *pos_proxy* and *act_horizon_expected_pos_diff* variables.
 - Data Type: \mathbb{R}^2
 - Structural Equation: $pos_proxy + act_horizon_expected_pos_diff$
- *act_horizon_target_pos*
 - Description: Target position by the end of the actuation horizon, derived the *lane_val_goal* and *act_horizon_expected_pos* variables.
 - Data Type: \mathbb{R}^2
 - Structural Equation: Projects the supplied position onto the closest point of the central path of the specified lane.
- *neg_pos*
 - Description: Negation of the *pos* variable.
 - Data Type: \mathbb{R}^2
 - Structural Equation: $-pos$
- *act_horizon_target_pos_diff*
 - Description: Target position difference by the end of the actuation horizon, calculated as the sum of the *act_horizon_target_pos* and *neg_pos* variables.
 - Data Type: \mathbb{R}^2
 - Structural Equation: $act_horizon_target_pos + neg_pos$
- *act_horizon_ang_sin*
 - Description: Sin of the angle between the position differences via the exterior product and sine rule for the *act_horizon_expected_pos_diff* and *act_horizon_target_pos_diff* variables.
 - Data Type: \mathbb{R}
- Structural Equation:
 - $act_horizon_expected_pos_diff[1] \times$
 - $act_horizon_target_pos_diff[0] +$
 - $act_horizon_expected_pos_diff[0] \times$
 - $act_horizon_target_pos_diff[1]$
- *act_horizon_ang_cos*
 - Description: Cosine of the angle between the position differences via the dot product and cosine rule for the *act_horizon_expected_pos_diff* and *act_horizon_target_pos_diff* variables.
 - Data Type: \mathbb{R}^2
 - Structural Equation: $\langle act_horizon_expected_pos_diff, act_horizon_target_pos_diff \rangle$
- *act_horizon_ang_cos_recip*
 - Description: Reciprocal of the *act_horizon_ang_cos* variable.
 - Data Type: \mathbb{R}
 - Structural Equation: $act_horizon_ang_cos^{-1}$
- *act_horizon_ang*
 - Description: Approximates the needed angle change for the actuation horizon via the tangent calculated from the product of the *act_horizon_ang_sin* and *act_horizon_ang_cos_recip* variables.
 - Data Type: \mathbb{R}
 - Structural Equation: $act_horizon_ang_sin \times act_horizon_ang_cos_recip$
- *ang_diff*
 - Description: Negation of the *act_horizon_ang* variable.
 - Data Type: \mathbb{R}
 - Structural Equation: $-act_horizon_ang$
- *ang_diff_buff*
 - Description: Buffer for the *ang_diff* variable.
 - Data Type: \mathbb{R}
 - Structural Equation: $f_{V_B}(ang_diff)$
- *prev_ang_diff*
 - Description: Represents the *ang_diff* variable for the previous time step via the *ang_diff_buff* variable.
 - Data Type: \mathbb{R}
 - Structural Equation: $f_{V_s}(ang_diff_buff)$
- *neg_prev_ang_diff*
 - Description: Negation of the *prev_ang_diff* variable.
 - Data Type: \mathbb{R}
 - Structural Equation: $-prev_ang_diff$
- *ang_diff_diff*
 - Description: Difference of angle differences between time steps, derived from the *ang_diff* and *neg_prev_ang_diff* variables.
 - Data Type: \mathbb{R}
 - Structural Equation: $ang_diff + neg_prev_ang_diff$
- *p_factor*

- Description: Proportional component of the PD controller derived from the *ang_diff* and *k_p* variables.
- Data Type: \mathbb{R}
- Structural Equation: $ang_diff \times k_p$
- *d_factor*
 - Description: Derivative component of the PD controller derived from the *ang_diff_diff* and *k_d* variables.
 - Data Type: \mathbb{R}
 - Structural Equation: $ang_diff_diff \times k_d$
- *needed_steer*
 - Description: Needed steer derived from the sum of the *p_factor* and *d_factor* variables.
 - Data Type: \mathbb{R}
 - Structural Equation: $p_factor + d_factor$
- *max_lim_steer*
 - Description: Maximum limited steer, via the *needed_steer* and *max_steer* variables.
 - Data Type: \mathbb{R}
 - Structural Equation: $\min\{needed_steer, max_steer\}$
- *actual_steer*
 - Description: Maximum & minimum limited steer, via the *max_lim_steer* and *min_steer* variables.
 - Data Type: \mathbb{R}
 - Structural Equation: $\max\{max_lim_steer, min_steer\}$

A.12 Full Control FWD Car

Description Simply a wrapper SCM that inherits from both *Motor Torque Control FWD Car* and *Steer Control FWD Car* SCMs. These SCMs combined are able to take a goal speed and goal lane id, along with target times by which to accomplish these goals, and in turn output motor torque and steer values for the associated *FWD Car* SCM.

Graphical Layout N/A

Variables N/A

A.13 Greedy Plan Pedestrian

Description Plans the next action for a *Goal Force Control Pedestrian* SCM specified as goals. In order to do so, a range of candidate nodes and target times are calculated and combined to form a variety of possible actions. The outcomes associated with taking these possible actions are then simulated, and the rewards associated with the action-outcome pairs are calculated. This does rely upon predefined a predefined simulator and predefined reward calculator being provided to the *Greedy Plan Pedestrian* SCM. In any case, once the rewards have been calculated the action associated with the maximum reward is selected and fed into the corresponding *Goal Force Control Pedestrian* SCM.

Graphical Layout Fig. 14 illustrates the graphical layout of the *Greedy Plan Pedestrian* SCM.

Variables

Hidden Exogenous:

- *time_horizon*
 - Description: Greatest duration ahead in seconds for goal times.
 - Data Type: \mathbb{R}
 - Distribution: $\langle \text{initialisation parameter} \rangle$
- *time_interval*
 - Description: Duration in seconds of intervals between goal times.
 - Data Type: \mathbb{R}
 - Distribution: $\langle \text{initialisation parameter} \rangle$
- *sim_params*
 - Description: Parameters for pedestrian domain simulation.
 - Data Type: PedSimParams
 - Distribution: $\langle \text{initialisation parameter} \rangle$
- *reward_params*
 - Description: Parameters for assessing reward within the pedestrian domain.
 - Data Type: PedRewardParams
 - Distribution: $\langle \text{initialisation parameter} \rangle$

Socket:

- *action*
 - Description: Output action from planner for pedestrian. Will be connected to *best_action* upon planner initialisation.
 - Data Type: $\mathbb{Z} \times \mathcal{T}$
 - Default Distribution: $Degenerate([0, 0]^T)$
- *pos*
 - Description: Pedestrian position.
 - Data Type: \mathbb{R}^2
 - Default Distribution: $Degenerate([0, 0]^T)$

Endogenous:

- *time_horizon_proxy*
 - Description: Proxy for the *time_horizon* variable.
 - Data Type: \mathbb{R}
 - Structural Equation: *time_horizon*
- *time_options*
 - Description: Range of goal time options based upon the current time, the *time_horizon_proxy* variable and the *time_interval* variable.
 - Data Type: 2^T
 - Structural Equation: Generates a range of candidate goal times starting at the current time and increasing by the specified time interval each candidate until reaching the specified horizon.
- *node*

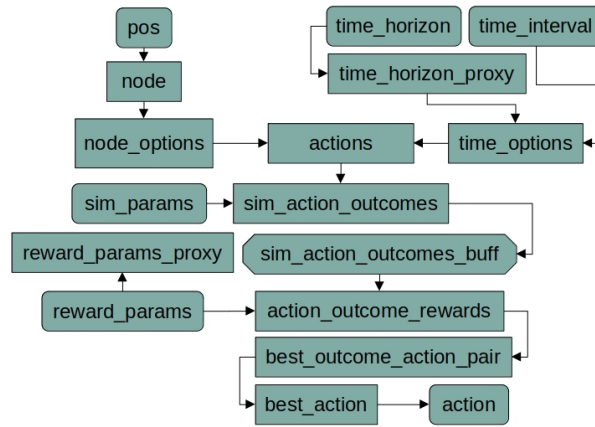


Figure 14: Greedy Plan Pedestrian SCM

- Description: Node associated with the position given by the pos variable.
- Data Type: \mathbb{Z}
- Structural Equation: Retrieves node id for node associated with the specified position by looking at the graphical roadmap.
- $node_options$
 - Description: Nodes accessible from the node specified by the $node$ variable.
 - Data Type: $2^{\mathbb{Z}}$
 - Structural Equation: Retrieves node associated with the specified node id from the graphical roadmap before returning its neighbours along with the node itself.
- $actions$
 - Description: Collection of candidate actions generated from the $time_options$ and $node_options$ variables.
 - Data Type: $2^{\mathbb{Z} \times \mathcal{T}}$
 - Structural Equation: $\{ [N, T]^{\top} \mid N \in \mathbb{Z}, T \in \mathcal{T} \}$
- $sim_action_outcomes$
 - Description: Provides a set of candidate actions and their associated outcomes using the $actions$ and sim_params variables.
 - Data Type: $2^{\text{Outcome} \times (\mathbb{Z} \times \mathcal{T})}$
 - Structural Equation: For each candidate action simulates the outcome of taking that action based upon the provided simulation parameters.
- $sim_action_outcomes_buff$
 - Description: Buffer for the $sim_action_outcomes$ variable.
 - Data Type: $2^{\text{Outcome} \times (\mathbb{Z} \times \mathcal{T})}$
 - Structural Equation: $f_{V_B}(sim_action_outcomes)$
- $reward_params_proxy$
 - Description: Proxy for the $reward_params$ variable.
 - Data Type: PedRewardParams
 - Structural Equation: $reward_params$

- $action_outcome_rewards$
 - Description: Calculates rewards associated with outcome-action pairs using the $sim_action_outcomes_buff$ and $reward_params$ variables.
 - Data Type: $2^{\mathbb{R} \times \text{Outcome} \times (\mathbb{Z} \times \mathcal{T})}$
 - Structural Equation: For each outcome-action pair calculates the associated reward based upon the provided reward parameters.
- $best_outcome_action_pair$
 - Description: Best outcome-action pair in terms of reward from the $action_outcome_rewards$ variable.
 - Data Type: $\text{Outcome} \times (\mathbb{Z} \times \mathcal{T})$
 - Struc. Eq.: $(\arg \max_{X \in action_outcome_rewards} X[0])[1:2]$
- $best_action$
 - Description: Gets the action part of the $best_outcome_action_pair$ variable.
 - Data Type: $\mathbb{Z} \times \mathcal{T}$
 - Structural Equation: $best_outcome_action_pair[1]$

A.14 Greedy Plan FWD Car

Description Plans the next action for a *Full Control FWD Car* SCM specified as goals. Effectively identical to the *Greedy Plan Pedestrian* SCM except for the format of the actions / goals, and the nature of the predefined simulators and reward calculators used by the SCM. Similar to the *Greedy Plan Pedestrian* SCM once the maximum reward action is selected it will be fed into the corresponding *Full Control FWD Car* SCM.

Graphical Layout Fig. 15 illustrates the graphical layout of the *Greedy Plan FWD Car* SCM.

Variables

Hidden Exogenous:

- $time_horizon$
 - Description: Greatest duration ahead in seconds for goal times.

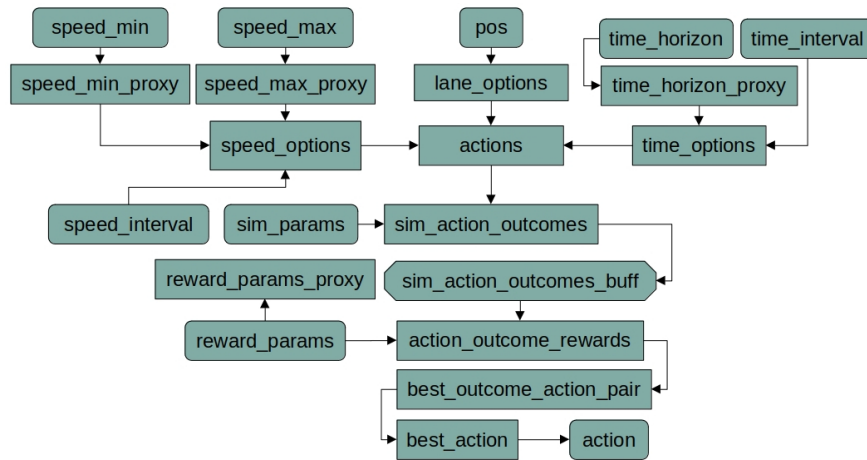


Figure 15: Greedy Plan FWD Car SCM

- Data Type: \mathbb{R}
- Distribution: $\langle \text{initialisation parameter} \rangle$
- *time_interval*
 - Description: Duration in seconds of intervals between goal times.
 - Data Type: \mathbb{R}
 - Distribution: $\langle \text{initialisation parameter} \rangle$
- *speed_min*
 - Description: Minimum speed goal value.
 - Data Type: \mathbb{R}
 - Distribution: $\langle \text{initialisation parameter} \rangle$
- *speed_max*
 - Description: Maximum speed goal value.
 - Data Type: \mathbb{R}
 - Distribution: $\langle \text{initialisation parameter} \rangle$
- *speed_interval*
 - Description: Speed goal value interval.
 - Data Type: \mathbb{R}
 - Distribution: $\langle \text{initialisation parameter} \rangle$
- *sim_params*
 - Description: Parameters for vehicle domain simulation.
 - Data Type: FWDCarSimParams
 - Distribution: $\langle \text{initialisation parameter} \rangle$
- *reward_params*
 - Description: Parameters for assessing reward within the vehicle domain.
 - Data Type: FWDCarRewardParams
 - Distribution: $\langle \text{initialisation parameter} \rangle$

Socket:

- *action*
 - Description: Output action from planner for vehicles. Will be connected to *best.action* upon planner initialisation.
 - Data Type: $(\mathbb{R} \times \mathcal{T}) \times (\mathbb{Z} \times \mathcal{T})$
 - Default Distribution: $Degenerate(\llbracket [0, 0]^\top, [0, 0]^\top \rrbracket)$
- *pos*
 - Description: Vehicle position.
 - Data Type: \mathbb{R}^2
 - Default Distribution: $Degenerate(\llbracket [0, 0]^\top \rrbracket)$

Endogenous:

- *time_horizon_proxy*
 - Description: Proxy for the *time_horizon* variable.
 - Data Type: \mathbb{R}
 - Structural Equation: *time_horizon*
- *time_options*
 - Description: Range of goal time options based upon the current time, the *time_horizon_proxy* variable and the *time_interval* variable.
 - Data Type: $2^{\mathcal{T}}$
 - Structural Equation: Generates a range of candidate goal times starting at the current time and increasing by the specified time interval each candidate until reaching the specified horizon.
- *speed_min_proxy*
 - Description: Proxy for the *speed_min* variable.
 - Data Type: \mathbb{R}
 - Structural Equation: *speed_min*
- *speed_max_proxy*
 - Description: Proxy for the *speed_max* variable.
 - Data Type: \mathbb{R}
 - Structural Equation: *speed_max*

- *speed_options*
 - Description: Range of speed goal value options based upon the *speed_min_proxy*, *speed_max_proxy*, and *speed_interval* variables.
 - Data Type: $2^{\mathcal{R}}$
 - Structural Equation: Generates a range of candidate speed goal values starting at the minimum speed and increasing by the specified speed interval each candidate until reaching the specified maximum speed.
- *lane_options*
 - Description: Range of lane goal value options based upon the *pos* variable.
 - Data Type: $2^{\mathcal{Z}}$
 - Structural Equation: Generates a range of candidate lane goal values by determining which lanes are within range and valid targets given the specified vehicle position.
- *actions*
 - Description: Collection of candidate actions generated from the *time_options*, *speed_options*, and *lane_options* variables.
 - Data Type: $2^{(\mathbb{R} \times \mathcal{T}) \times (\mathbb{Z} \times \mathcal{T})}$
 - Structural Equation: $\{ [[S, T]^{\top}, [L, T']^{\top}] \mid S \in \mathbb{R}, L \in \mathbb{Z}, T, T' \in \mathcal{T} \}$
- *sim_action_outcomes*
 - Description: Provides a set of candidate actions and their associated outcomes using the *actions* and *sim_params* variables.
 - Data Type: $2^{\text{Outcome} \times ((\mathbb{R} \times \mathcal{T}) \times (\mathbb{Z} \times \mathcal{T}))}$
 - Structural Equation: For each candidate action simulates the outcome of taking that action based upon the provided simulation parameters.
- *sim_action_outcomes_buff*
 - Description: Buffer for the *sim_action_outcomes* variable.
 - Data Type: $2^{\text{Outcome} \times ((\mathbb{R} \times \mathcal{T}) \times (\mathbb{Z} \times \mathcal{T}))}$
 - Structural Equation: $f_{V_B}(\text{sim_action_outcomes})$
- *reward_params_proxy*
 - Description: Proxy for the *reward_params* variable.
 - Data Type: FWDCarRewardParams
 - Structural Equation: *reward_params*
- *action_outcome_rewards*
 - Description: Calculates rewards associated with outcome-action pairs using the *sim_action_outcomes_buff* and *reward_params* variables.
 - Data Type: $2^{\mathbb{R} \times \text{Outcome} \times ((\mathbb{R} \times \mathcal{T}) \times (\mathbb{Z} \times \mathcal{T}))}$
 - Structural Equation: For each outcome-action pair calculates the associated reward based upon the provided reward parameters.
- *best_outcome_action_pair*

- Description: Best outcome-action pair in terms of reward from the *action_outcome_rewards* variable.
- Data Type: $\text{Outcome} \times ((\mathbb{R} \times \mathcal{T}) \times (\mathbb{Z} \times \mathcal{T}))$
- Struc. Eq.: $(\arg \max_{X \in \text{action_outcome_rewards}} X[0])[1:2]$
- *best_action*
 - Description: Gets the action part of the *best_outcome_action_pair* variable.
 - Data Type: $(\mathbb{R} \times \mathcal{T}) \times (\mathbb{Z} \times \mathcal{T})$
 - Structural Equation: *best_outcome_action_pair*[1]

References

- Blum, E. K.; and Lototsky, S. V. 2006. *Mathematics of physics and engineering*. World Scientific Publishing Company.
- Guiggiani, M. 2018. *The Science of Vehicle Dynamics: Handling, Braking, and Ride of Road and Race Cars*. Springer.
- Helbing, D.; and Molnár, P. 1995. Social force model for pedestrian dynamics. *Phys. Rev. E*, 51: 4282–4286.
- Lipták, B. G. 2013. *Process Control: Instrument Engineers' Handbook*. Butterworth-Heinemann.
- Nahata, R.; Omeiza, D.; Howard, R.; and Kunze, L. 2021. Assessing and Explaining Collision Risk in Dynamic Environments for Autonomous Driving Safety. In *2021 IEEE International Intelligent Transportation Systems Conference (ITSC)*, 223–230.